EQUILIBRATION OF A LIQUID DROPLET - VAPOR - GAS MIXTURE DOWNSTREAM OF A SHOCK WAVE

Thesis by

Robert Rosen

In Partial Fulfillment of the Requirements

For the Degree of

Mechanical Engineer

California Institute of Technology

Pasadena, California

1966

ACKNOWLEDGMENTS

The author wishes to express his appreciation to his thesis advisor, Professor Frank E. Marble, whose guidance made this work most enjoyable.

ABSTRACT

The equations of motion for the flow of a mixture of liquid droplets, their vapor, and an inert gas through a normal shock wave are derived. A set of equations is obtained which is solved numerically for the equilibrium conditions far downstream of the shock. The equations describing the process of reaching equilibrium are also obtained. This is a set of first-order nonlinear differential equations and must also be solved numerically. The detailed equilibration process is obtained for several cases and the results are discussed.

TABLE OF CONTENTS

I. INTRODUCTION

In recent years considerable attention has been focussed on flows of particle-laden fluids. This interest has been stumulated by the occurrence of many relevant physical situations, among which is the problem of solid particles in the exhaust of a metalized solid-propellant rocket motor.

One of the fundamental and tractable problems of high speed flow is the structure of the normal shock wave. Carrier[1] undertook the original investigation of shock waves involving small particles, in which he solved the problem of the flow of a gas and a cloud of uniform sized solid particles through a normal shock wave. Since the problem was essentially nonlinear, a closed form solution was impossible and he illustrated the relaxation process by calculating a few sample cases. The physical phenomena, however, were neither clear nor were they examined thoroughly. Marble[2] expanded Carrier's work by extending and varying the range of the physical variables and interpreting the results in terms of a physical process related to certain characteristic parameters. Further extension of solutions to the shock wave problem was carried out by Rudinger[3], in which he studied the structure of the relaxation zone for various shock strengths and the thermodynamic properties of the gas and solid. He also studied the effect of the particle drag law and found that the approach to equilibrium was highly dependent on this law. Variation in Nusselt number, however, was much less significant. For the limiting case of weak shock waves and a single particle size,

Kriebel[4] obtained the closed form solution and presented a technique for numerically integrating the equations for a discrete distribution of particle sizes.

In spite of this interest in shock structure for heterogeneous media, the same problem has not been investigated for volatile liquid particles. Flows of this sort have for many years been known to occur in some stages of vapor cycle turbomachinery, in liquid metal loops, as well as in the early part of rocket nozzle flow. Knowledge of such flows also affords a possible means of measuring the quality of vapor-gas streams in general.

It is the purpose of this thesis to investigate the approach to dynamic and thermodynamic equilibrium of liquid droplets passing through a shock wave, the gas consisting of vapor and inert gas. This problem is somewhat more difficult than the analogous problem for solid particles because another condition for equilibrium must be taken into account; equilibrium between the liquid and its vapor phase. It will be assumed that upstream of the shock wave a uniform distribution of single size, spherical liquid droplets exists in the flow. These droplets have the same velocity and temperature as the gas-vapor mixture. Furthermore, the concentration of vapor in the gas is such that thermodynamic equilibrium exists between the liquid and vapor phases; this will be designated an equilibrium state. Far downstream, it is assumed that another equilibrium state exists.

It is assumed further that there are no interactions between the individual particles, that the wakes of particles do not affect the

flow around nearby particles, and that Stokes drag law may be used in the momentum equation. Heat exchange between gas and liquid is by convection only; radiative transfer between particles or from particles to gas is neglected. The fluid is considered inviscid except in the shock wave and the portion of the flow that produces the particle drag. Finally, the liquid temperature in a particle is assumed uniform. The liquid mass fractions are such that the volume occupied by the particles is negligible, and any changes in density of the fluid do not affect the size of the droplets directly. Other assumptions will be stated at the time they are required.

In order to avoid confusion in the following work, a definite distinction has been made between the terms fluid, gas, and vapor. The term 'fluid' will refer only to the mixture of two substances in which the particles flow. The term 'gas' will only be used for the inert component of the fluid, i.e., the one which does not exchange mass with the droplets. Finally, the 'vapor' is the component of the fluid which exchanges mass with the particles.

II. FORMULATION OF THE SHOCK-RELAXATION PROBLEM

The equations describing the flow can be derived from two points of view. One concerns the overall conservation of mass, momentum, and energy between points separated by a finite distance. This leads to a set of algebraic equations which can be solved to yield the flow conditions far downstream of the shock. The other point of view is a more detailed one involving the interchange of mass, momentum, and energy between the particles and fluid. This leads to a set of differential equations which give the nature of the equilibration process. The former viewpoint will be employed first.

The Overall Conservation Relations

Consider a control volume which extends between any two points in a flow. Since the flow is one-dimensional, steady, and without mass addition, continuity demands that the total flux of mass in the x-direction into the control volume be equal to the flux out, and both of the quantities are constant. Thus,

$$\rho u + \rho_p u_p = \text{constant.}$$

It is necessary to deal with the total mass because there is an exchange between the particles and fluid in the form of condensation or evaporation of vapor. If we evaluate the constant at a location where the particles and gas-vapor mixture are in equilibrium, we have

$$\rho u + \rho_p u_p = (\rho_1 + \rho_{p1}) u_1 \quad , \tag{1}$$

and if both states are equilibrium states,

$$(\rho_1 + \rho_{p1}) u_1 = (\rho_3 + \rho_{p3}) u_3 \quad .$$

An equilibrium state is one for which the velocity and temperature of the particles are equal to those of the fluid, and the liquid of the particles is in thermodynamic equilibrium with its vapor in the mixture. The component of the mixture which plays no active role in the evaporation or condensation has an equation of continuity of its own, which is

$$\rho_g u = \text{const} = \rho_{g1} u_1 \quad .$$

Since

$$\rho = \rho_g + \rho_v \, ,$$

we have

$$\rho u\left(1 - \frac{\rho_v}{\rho}\right) = \rho_1 u_1 \left(1 - \frac{\rho_{v1}}{\rho_1}\right) \, ,$$

or

$$\rho u(1 - K_v) = \rho_1 u_1 (1 - K_{v1}) \, . \qquad (2)$$

Considering this between states 1 and 3, we have

$$\frac{\rho_3 u_3}{\rho_1 u_1} = \frac{1-K_{v1}}{1-K_{v3}}$$

We define δ as the ratio of mass flux of fluid far downstream of the shock to mass flux of fluid upstream, that is,

$$\delta \equiv \frac{\rho_3 u_3}{\rho_1 u_1} \quad .$$

An equation, similar to equation (2), expressing the particle mass flux in terms of the vapor concentration and known conditions at another location can easily be obtained from (1) and (2). It is

$$\rho_p u_p = \rho_{p1} u_1 + \rho_1 u_1 \left(\frac{K_{v1} - K_v}{1 - K_v} \right) .$$

The equilibrium value of the concentration will be of interest and can be determined from the Clausius-Clapeyron equation,

$$\frac{dp}{dT} = \frac{h_\ell}{T(v_g - v_\ell)} .$$

Neglecting the specific volume of the liquid compared to that of the vapor and using the perfect gas law, this becomes

$$\frac{dp}{dT} = \frac{h_\ell p}{RT^2} .$$

Integration gives

$$p_s = e^{-\frac{h_\ell}{RT} + c}$$

where the subscript indicates the saturation pressure, and c is a constant of integration. Now

$$K_v^e = \frac{p_s R}{p R_v} .$$

Thus,

$$\frac{K_v^e}{K_{v1}^e} = \frac{p_1}{p} \exp\left[- \frac{h_\ell}{RT_1} \left(\frac{T_1}{T_p} - 1 \right) \right] \qquad (4)$$

The law of conservation of momentum states that the net force on a control volume in the x-direction is equal to the rate of change of x momentum inside. The rate of change of momentum inside the control volume is the difference between the momentum leaving and entering. The net force is just the difference in pressure. Hence,

$$p_1 - p = \rho u^2 + \rho_p u_p^2 - \rho_1 u_1^2 - \rho_{p1} u_1^2 ,$$

or

$$\rho u^2 + \rho_p u_p^2 + p = (\rho_1 + \rho_{p1})u_1^2 + p_1 \qquad (5)$$

where use has been made of the fact that state 1 is an equilibrium state.

In a similar manner the energy equation is found to be

$$\rho u(c_p T + h_\ell + \tfrac{1}{2}u^2) + \rho_p u_p(cT_p + \tfrac{1}{2}u_p^2) = \rho_1 u_1(c_p T_1 + h_\ell + \tfrac{1}{2}u_1^2) + \rho_{p1} u_{p1}(cT_1 + \tfrac{1}{2}u_1^2) \; . \qquad (6)$$

Here, the term $\rho u h_\ell$ accounts for the fact that energy is absorbed in the form of latent heat during vaporization.

Upon the assumption that the gas-vapor mixture acts as a perfect gas, we have the usual equation of state,

$$p = \rho R T \; . \qquad (7)$$

These seven equations are now sufficient to completely determine the equilibrium state far downstream of the shock. This will be done in Section III.

Before going on to derive the differential equations which describe the equilibration zone, it is convenient to derive an equation for the particle radius. The continuity equation can be written as

$$\frac{\rho_p u_p}{\rho_{p1} u_1} = 1 + \frac{\rho_1}{\rho_{p1}} - \frac{\rho u}{\rho_{p1} u_1}$$

or

$$\frac{\rho_p u_p}{\rho_{p1} u_1} = 1 + \frac{1}{K_{p1}} - \frac{\rho u}{\rho_1 u_1}\frac{\rho_1}{\rho_{p1}}$$

where $K_{p1} = \rho_{p1}/\rho_1$. Now $\rho_p = nm$, and for spherical particles, $m = \frac{4}{3}\pi\sigma^3\rho_\ell$. Hence

$$\frac{\sigma^3 n u_p}{\sigma_1^3 n_1 u_{p1}} = 1 + \frac{1}{K_{p1}}\left(1 - \frac{\rho u}{\rho_1 u_1}\right) ,$$

where it has been assumed that all the particles at any location have the same radius. It has been assumed that no particles are created or destroyed. This implies a conservation of number flux of particles,

$$\frac{d}{dx}(nu_p) = 0 ,$$

or

$$nu_p = n_1 u_{p1} .$$

Using the above gives finally,

$$\left(\frac{\sigma}{\sigma_1}\right)^3 = 1 + \frac{1}{K_{p1}}\left(1 - \frac{\rho u}{\rho_1 u_1}\right) . \qquad (8)$$

Relations Governing Relaxation Zone

We now proceed to derive the differential equations describing the particle motion. Consider a control volume of length dx and of unit height and width sufficiently large that the assumption of a particle continuum is valid. The increase of the mass rate of flow of particles in the control volume is readily found to be $\frac{d}{dx}(\rho_p u_p)dx$. This must be equal to the rate of mass absorbed by all the particles in the control volume. The number of particles in the control volume is $n\,dx$, and if $\dot{m}$ is the rate of mass given off by each, $-\dot{m}n\,dx$ is the rate of mass absorbed. Thus,

$$\frac{d}{dx}(\rho_p u_p)dx = -\dot{m}n\,dx .$$

w is defined as the rate of mass given off by all the particles per unit volume. Hence,

$$\frac{d}{dx}(\rho_p u_p) = - w \quad . \tag{9}$$

From continuity it is obvious that

$$\frac{d}{dx}(\rho u) = w \quad .$$

It will be more convenient later on to have K_v as the dependent variable rather than $\rho_p u_p$. We can write the above equation as

$$\frac{d}{dx}(\rho_g u + \rho_v u) = w \quad .$$

Since $\rho_g u = \text{const}$, this reduces to

$$\frac{d}{dx}(\rho u K_v) = w \quad .$$

Expanding the derivative and rearranging gives

$$\rho u \frac{dK_v}{dx} = (1 - K_v)w \quad . \tag{10}$$

The change of momentum of the particles in the control volume is equal to the drag on the particles minus the amount of momentum that leaves the particles with the evaporating vapor. The change of momentum is simply $\frac{d}{dx}(\rho_p u_p^2)dx$. If the drag force on each particle is given by Stokes law, then the momentum change due to drag on all the particles is

$$-6\pi n\mu\sigma(u_p - u)dx \quad .$$

The physical model under consideration assumes that, except very close to the particles, the fluid velocity is uniform. This means that the velocity of any evaporated vapor must change rapidly to that of the free stream. It will be assumed that the force necessary to change the velocity of the vapor to that of the free stream acts entirely on the particles. Thus, the momentum taken away by the evaporating vapor in the control volume is $n\dot{m}udx$. Combining these terms

and simplifying gives

$$\frac{d}{dx}(\rho_p u_p^2) = -wu - 6\pi n\mu\sigma(u_p - u) \ .$$

After expanding the derivative, using equation (9) and simplifying the results,

$$\rho_p u_p \frac{du_p}{dx} = w(u_p - u) - 6\pi n\mu\sigma(u_p - u) \ . \qquad (11)$$

In a similar manner, the energy equation for the particles is obtained. The rate of change of energy is equal to the rate of heat transferred from the gas to the particles minus the rate of energy transported away by the evaporating vapor. As with the momentum, it is assumed that when the vapor leaves the particles, it has the same temperature as the fluid and has gotten the necessary energy from the particles. Using these facts and simplifying the resulting equation in a similar fashion to what was done for the momentum equation gives

$$\rho_p u_p c \frac{dT_p}{dx} = - w[h_\ell + c_p(T - T_p)] - H \ ,$$

where H is the total rate of heat transfer from the particles to the gas. Reference 2 points out that the Nusselt number, $\sigma h/k$, is unity when Stokes drag law is a valid approximation. Hence, the equation becomes

$$\rho_p u_p c \frac{dT_p}{dx} = -w[h_\ell + c_p(T - T_p)] - 4n\pi k\sigma(T_p - T) \ . \qquad (12)$$

From Frick's law,

$$\dot{m} = -\rho h_D A_s (K_v - K_v^e) \ .$$

By the analogy between heat and mass transfer,

$$h_D = \frac{Dh}{k} ,$$

so

$$\dot{m} = -4\pi\sigma\rho D(K_v - K_v^e)$$

and

$$w = -4n\pi\sigma\rho D(K_v - K_v^e) . \tag{13}$$

The characteristic time for changes in velocity, as shown in reference 2, is

$$\tau_r = \frac{m(u_p - u)}{F} = \frac{m}{6\pi\sigma\mu} .$$

The velocity range, which is the characteristic length for changes in velocity, is found by reference 2 as

$$\lambda_v = \frac{ma}{6\pi\sigma\mu} . \tag{14}$$

In a similar manner, the thermal range and diffusion range were found to be

$$\lambda_T = \frac{mac}{4\pi\sigma k} \tag{15}$$

and

$$\lambda_D = \frac{ma}{4\pi\sigma\rho D} , \tag{16}$$

respectively. The speed of sound varies as the one-half power of the temperature for a perfect gas, and the viscosity goes as the three-fourths power. Thus, for small changes in temperature, the ratio a/μ is almost constant. In this work it will be assumed constant. With this in mind, equation (14) becomes

$$\lambda_v = \text{const } \sigma^2 ,$$

or

$$\frac{\lambda_v}{\lambda_{v3}} = \Sigma \ ,$$

where $\Sigma = \left(\frac{\sigma}{\sigma_3}\right)^2$. Likewise, (15) reduces to

$$\frac{\lambda_T}{\lambda_{T3}} = \Sigma$$

if, in addition to a/μ , the Prandtl number is constant. Finally, upon assuming the Schmidt number is also constant, (16) can be written as

$$\frac{\lambda_D}{\lambda_{D3}} = \Sigma$$

Using the definitions of λ_v , λ_T , and λ_D and equation (13), we obtain the following set of differential equations:

$$\frac{d}{dx}(\rho_p u_p) = \frac{\rho_p a}{\lambda_{D3}\Sigma}(K_v - K_v^e) \tag{17}$$

$$\rho u \frac{dK_v}{dx} = -\frac{\rho_p a}{\lambda_{D3}\Sigma}(1-K_v)(K_v - K_v^e) \tag{18}$$

$$\rho_p u_p \frac{du_p}{dx} = -\frac{\rho_p a}{\lambda_{v3}\Sigma}\left[1+\frac{\lambda_{v3}}{\lambda_{D3}}(K_v - K_v^e)\right](u_p - u) \tag{19}$$

$$\rho_p u_p c \frac{dT_p}{dx} = -\frac{\rho_p ac}{\lambda_{T3}\Sigma}\left[1 + \frac{\lambda_{T3}}{\lambda_{D3}}(K_v - K_v^e)\right](T_p - T) + \frac{h_\ell a}{\lambda_{D3}\Sigma}(K_v - K_v^e) \tag{20}$$

and

$$w = -\frac{\rho_p a}{\lambda_{D3}\Sigma}(K_v - K_v^e) \ . \tag{21}$$

Equations (17) or (18) and (19) and (20) fully describe the motion of the particles. The solution of these equations will be obtained in Section IV. A set similar but pertaining to the motion of the gas can be arrived at by differentiating the overall conservation equations

and eliminating the unwanted differential quantities with the aid of the above equations.

III. DOWNSTREAM EQUILIBRIUM CONDITIONS

The normal shock relations for the conditions downstream of a shock wave in a perfect gas can be found in any text on gas dynamics. In much the same way, the equilibrium conditions for state 3 have been determined in this work. It will be seen that a difference exists between these two sets of equations, for in the present instance an explicit solution is not possible.

Formulation of the Downstream Conditions

It is assumed that the physical properties of the gas (R, c_p, etc.) are constant and are equal to those of the vapor, and that the specific heat per unit mass of the liquid drops is equal to the specific heat of the gas-vapor mixture. While this assumption simplifies the algebraic manipulations, it changes neither the fundamental mathematics of the problem nor the physics of the situation.

Writing the momentum equation between states 1 and 3, dividing by p_1 and rearranging yields

$$\frac{p_3}{p_1} = 1 + \frac{(\rho_1+\rho_{p1})u_1^2}{p_1}\left(1 - \frac{u_3}{u_1}\right) .$$

By making use of the definition of the Mach number, this can be written as

$$\frac{p_3}{p_1} = 1 + \gamma M_1^2 (1+K_{p1})\left(1 - \frac{u_3}{u_1}\right) \qquad (22)$$

Between these states the energy equation, equation (6), can be written as

$$c_p T_3 + \tfrac{1}{2}u_3^2 = c_p T_1 + \tfrac{1}{2}u_1^2 - \frac{h_\ell}{1+K_{p1}}(\delta-1) .$$

Upon eliminating the temperature in terms of the pressure and dividing by $a_1^2/(\gamma-1)$, there results

$$\frac{p_3}{p_1}\frac{u_3}{u_1}\frac{1}{\delta}+\frac{\gamma-1}{2}M_1^2\frac{u_3^2}{u_1^2}=1+\frac{\gamma-1}{2}M_1^2-\frac{\gamma-1}{a_1^2}\frac{h_\ell}{1+K_{p1}}(\delta-1) \quad .$$

Using equation (21) to eliminate p_3/p_1 and solving the resulting quadratic equation in u_3/u_1, the following expression for u_3/u_1 in terms of δ results:

$$\frac{u_3}{u_1}=\frac{1}{2\delta M_1^2\left[\frac{\gamma(1+K_{p1})}{\delta}-\frac{\gamma-1}{2}\right]}\left\{1+\gamma M_1^2(1+K_{p1})-\left[\left[1+\gamma M_1^2(1+K_{p1})\right]^2-\right.\right.$$
$$\left.\left.4\delta M_1^2\left[\frac{\gamma(1+K_{p1})}{\delta}-\frac{\gamma-1}{2}\right]\left[1+\frac{\gamma-1}{2}M_1^2-\frac{\gamma-1}{\gamma}\frac{\delta-1}{1+K_{p1}}\frac{h_\ell}{RT_1}\right]\right]^{\frac{1}{2}}\right\} \qquad (23)$$

The temperature ratio can be found in terms of the velocity ratio and δ. From the perfect gas law,

$$\frac{T_3}{T_1}=\frac{p_3}{p_1}\frac{\rho_1}{\rho_3} \quad ,$$

or

$$\frac{T_3}{T_1}=\frac{p_3}{p_1}\frac{u_3}{u_1}\frac{1}{\delta} \quad .$$

Hence,

$$\frac{T_3}{T_1}=\frac{1}{\delta}\frac{u_3}{u_1}\left[1+\gamma M_1^2(1+K_{p1})\left(1-\frac{u_3}{u_1}\right)\right] \quad . \qquad (24)$$

Utilizing the definition of δ in equation (2), there results

$$\delta=\frac{1-K_{v1}}{1-K_{v3}} \quad .$$

Solving for p_3/p_1 in the equation directly above equation (24), and substituting this into equation (4) gives

$$K_{v3} = \frac{K_{v1}(u_3/u_1)}{\delta(T_3/T_1)} \exp\left[\frac{h_\ell}{RT_1}\left(1 - \frac{T_1}{T_3}\right)\right] .$$

Combining these two and solving for δ results in

$$\delta = 1 - K_{v1}\left\{1 - \frac{(u_3/u_1)}{(T_3/T_1)} \exp\left[\frac{h_\ell}{RT_1}\left(1 - \frac{T_1}{T_3}\right)\right]\right\} . \qquad (25)$$

Equations (23), (24), and (25) are three algebraic equations in the three unknowns, u_3/u_1, T_3/T_1, and δ. These three quantities are uniquely determined and with them, the equilibrium conditions downstream of the normal shock wave. Due to the occurrence of the exponential term in equation (25), it is not possible to solve the system of equations explicitly, and, in fact, it was not found to be worthwhile to simplify them further.

Numerical Solution and Results

Although the unknowns cannot be determined explicitly, their solution is quite easy to obtain. It was found that the nature of the equations in the region of interest is such that even the most mundane numerical technique rapidly converges to the solution. The region of interest in terms of δ will later be shown to be $1-K_{v1} < \delta \leq 1+K_{p1}$.

Knowing these three quantities, the pressure ratio can be found from (22), the density ratio from

$$\frac{\rho_3}{\rho_1} = \frac{\delta}{(u_3/u_1)} ,$$

the particle density ratio from

$$\frac{\rho_{p3}}{\rho_{p1}} = \frac{1 + \frac{1-\delta}{K_{p1}}}{(u_3/u_1)} ,$$

and the particle radius from

$$\left(\frac{\sigma_3}{\sigma_1}\right)^3 = 1 + \frac{1-\delta}{K_{p1}} \quad .$$

The results of several calculations for various values of the Mach number, initial particle concentration, and non-dimensional latent heat, $\frac{h_\ell}{RT_1}$, are shown in Figures 1 through 9.

Inspection of these figures shows the somewhat surprising occurrence of δ less than one. This essentially means that in certain cases some of the vapor condenses onto the particles and that they grow in size as a result of the process of coming to equilibrium. Thus, the situation is somewhat more complex than would be expected from just considering the fact that the gas temperature is increased by going through the shock wave.

Discussion of the Results

An explanation of what is happening will begin with a description of the role of the parameter δ. As mentioned earlier, δ is the ratio of mass flow of fluid at state 3 to the mass flow of fluid at state 1. If δ is greater than one, mass had to be added to the gas-vapor stream. This mass could only have come from the particles, and it must have been in the form of evaporated vapor. Similarly, if δ is less than one, it means that some of the vapor that was travelling with the gas stream upstream of the shock must have been condensed onto the particles. Thus, δ is the indicator of whether evaporation or condensation has taken place, and, to a certain extent, how much.

There is a physical limit to how much vapor can evaporate or

condense. From this, it is a simple matter to put restrictions on the values of δ. By proper rearranging of the continuity equation, it is possible to write

$$\delta = \frac{1-K_{v1}}{1-K_{v3}} = \frac{1+K_{p1}}{1+K_{p2}} .$$

If we consider the case where the condensation is very great and no vapor remains in the flow at state 3, we have $\delta = 1-K_{v1}$. Since this corresponds to a condition where $K_{v3} = 0$, we see from equation (4), the expression determining the equilibrium concentration, that this is really impossible. It would require a zero temperature or an infinite pressure at state 3. Thus, it should be written as $\delta > 1-K_{v1}$. It is perfectly reasonable, however, to expect the final temperature to be so high that all of the liquid in the incoming particles evaporates. This, in fact, may actually happen, so δ may be equal to $1+K_{p1}$. Putting these together, we have the limits on δ mentioned on page 16.

There is one other special case involving δ. That is when δ has the value of unity. This means that the value of the final particle concentration is equal to the initial value, or that there is no net evaporation or condensation in the process. Since there is no net change in particle size or vapor concentration, the results are identical to those of non-volatile solid particles. It should be kept in mind that this is an overall effect, not a local one, so that at any point downstream of the shock wave but upstream of where the mixture reaches equilibrium again, the value of K_v is probably not K_{v1}. The conditions which must be met in order for δ to equal *unity can be* determined from equation (25). Inspection shows that for this to hold,

the quantity in the brackets must be zero, or

$$\frac{(u_3/u_1)}{(T_3/T_1)} \exp\left[\frac{h_\ell}{RT_1}\left(1 - \frac{T_1}{T_3}\right)\right] = 1 \ .$$

From equations (23) and (24) it can be seen that when δ equals 1, both u_3/u_1 and T_3/T_1 depend only on M_1 and K_{p1} (for fixed γ). Thus, the expression can be solved explicitly for $h_\ell/(RT_1)$ if desired. But, in general, given two of the three quantities M_1, K_{p1}, or $h_\ell/(RT_1)$, the above expression will determine the third, so that there is no difference in the particle concentration before and after the shock. It should be noted that this is independent of K_{v1}.

Since $\delta = 1$ separates the region in which there is vapor condensation from the region in which evaporation occurs, the value of the parameters which satisfy the above relationship is very important. These are the limiting values, with respect to condensation, of each parameter if the other two are held fixed. For example: the equation is satisfied by values of 1.6, .15, and 4.88 for M_1, K_{p1}, and $h_\ell/(RT_1)$, respectively. At this Mach number and initial particle concentration, condensation will occur if $h_\ell/(RT_1)$ is less than 4.88, and vapor will be evaporated if it is greater.

Figure 1 is a plot of δ versus K_{v1} for $M_1 = 1.6$, $K_{p1} = .15$, and various values of $h_\ell/(RT_1)$. On it are curves for which the particles grow $\left(h_\ell/(RT_1) = 2.5\right)$, shrink $\left(h_\ell/(RT_1) = 10.15\right)$, or remain the same as a result of passing through the shock wave. It can be seen that the relationship between δ and $h_\ell/(RT_1)$ is a complex one. It appears that for values of K_{v1} greater than .2, δ has a maximum

for a value of $h_\ell/(RT_1)$ somewhere between 4.88 and 15. This same phenomenon occurs for different values of the Mach number and initial particle concentration.

There is no particularly significant reason for assigning the role of independent variable in all these curves to K_{v1}. However, K_{v1} does have an important physical interpretation. It is the quantity that determines the magnitude of the equilibrium constant. Large values of K_{v1} imply a large equilibrium constant. Thus, the effects of condensation and evaporation are magnified by increasing K_{v1}. Later, a case will be discussed for which all the liquid in the particles vaporizes. This will only occur for values of K_{v1} above a certain value. This fact clearly shows the relationship between K_{v1} and the equilibrium constant. It is obvious that a zero value for K_{v1} corresponds to solid particles.

The quantity which determines whether or not δ will be greater or less than one is the final vapor concentration. If the ratio of this to the initial vapor concentration is greater than one, then δ will be also. The ratio of K_{v3} to K_{v1} is in turn determined by p_3/p_1 and T_3/T_1, as shown by equation (4).

The relationship between T_3/T_1 and K_{v1}, K_{p1}, $h_\ell/(RT_1)$, and M_1 can be seen from Figures 2 through 5. Figure 2 is a plot of T_3/T_1 against K_{v1} for $M_1 = 1.6$, $K_{p1} = .15$, and various values of $h_\ell/(RT_1)$. It should be noticed from the figure that T_3/T_1 is greater than one for all values of K_{v1} and $h_\ell/(RT_1)$. This was found to hold true in all the other calculations made for varying Mach number, ini-

tial particle concentration, and non-dimensional latent heat ratio. Forgetting for a moment that evaporation and condensation take place, this result is in line with intuitive feelings gained from a knowledge of normal shock waves in a perfect gas. The role that all the variables play in making this so is somewhat obscure, however. Just downstream of the shock the particles are still at T_1, but the fluid has been compressed to a higher temperature. If the final temperature was determined from just these two quantities, it would be obvious that T_3 should exceed T_1. The effect of the difference in particle and fluid velocity after the shock is not so clear. It is clear that the particles exert a force on the fluid which increases the fluid velocity. This in turn lowers the velocity of the particles. Since the total energy is a constant, these changes in kinetic energy produce changes in particle and fluid temperatures. Coupled with this is the kinetic energy converted to heat through viscous dissipation. The interrelation between all these effects in this complicated situation has not been studied in the necessary detail to determine the circumstances under which each is dominant.

The previous discussion pertains only to the line for which $\delta = 1$ or the point on the curves in the figures for which $K_{v1} = 0$, since it is for only these points that no evaporation or condensation occurs. The effect of the non-dimensional latent heat ratio can readily be seen from the other curves in the figure. If $h_\ell/(RT_1)$ is such that vapor condenses, then T_3/T_1 will be greater than if the particles were non-volatile. The explanation of this is as follows. The

condensing vapor gives off its latent heat to the fluid stream. This extra heat eventually raises the temperature of the whole mixture. Thus, the more vapor condensed, the higher T_3/T_1. Naturally, the opposite happens when vapor is evaporated from the particles. The heat necessary to change the phase of the liquid is no longer available to raise the final temperature. For the case of no condensation or evaporation, the latent heat has no effect. That is why the curve for $h_\ell/(RT_1) = 4.88$ (corresponding to $\delta = 1$) is a horizontal line in the figure. There is one slight correction to be made with what has been said thus far. From Figure 1 it can be seen that for K_{vl} greater than about .2, more mass is evaporated from the particles with a non-dimensional latent heat ratio of 10 than the particles with a ratio of 15. Yet T_3/T_1 is lower for the particles with an $h_\ell/(RT_1)$ of 15 than 10. This is undoubtedly due to the fact that only a couple of per cent more mass is evaporated from the particles with a latent heat ratio of 10, while the difference in latent heat ratio for the two cases is 50 per cent.

The same relationship between T_3/T_1 and $h_\ell/(RT_1)$ is illustrated in Figure 3. This curve is again for an initial Mach number of 1.6, but now K_{pl} is .05. The discontinuity in the slope of the curve for $h_\ell/(RT_1) = 10$ is caused by the complete evaporation of all the particles. For values of K_{vl} less than .054, everything happens as it did in Figure 2. A value of K_{vl} equal to .054 corresponds to a state where all the liquid has been evaporated but the gas is fully saturated with the vapor.

For any value of K_{v1} greater than .054, more vapor can be dissolved in the gas. However, there is no liquid left to vaporize, and the vapor becomes superheated. As long as all the liquid has been vaporized, the amount of energy converted into latent heat is the same. Thus, no difference in T_3/T_1 for two values of K_{v1} greater than .054 should be expected. This explains the zero slope for K_{v1} greater than .054. Of course, the same result can be obtained from the equations without this physical argument. For any value of K_{v1} greater than .054, all the liquid is vaporized. This corresponds to δ having its maximum value, $1+K_{p1}$. With δ known and fixed, u_3/u_1 is uniquely determined independent of K_{v1} by equation (23), and T_3/T_1 by equation (24). It should be noted that equation (25), which insures the equilibrium between the liquid and vapor, is no longer pertinent.

A better idea of how T_3/T_1 varies with K_{p1} can be obtained from Figure 4. In this plot, the conditions are such that δ is always greater than one. If this were plotted for δ less than one, the shape of the curves would be similar to those of Figures 2 and 3 for $h_\ell/(RT_1) = 2.5$. In that case, T_3/T_1 would also be greater for larger values of K_{p1}. It is believed that the increase of T_3/T_1 with K_{p1} is due to greater dissipation caused by a larger mass of liquid in the flow, be it in the form of larger particles or a greater number of particles, or both. This is why the same result occurs when $h_\ell/(RT_1)$ is 2.5 even though the vaporization process works in the opposite direction. Study of a curve of u_3/u_1 plotted against K_{v1}

for different values of K_{v1} bears this out. Here, u_3/u_1 is smaller for greater values of K_{p1}, even though the total momentum just past the shock is greater in the flow with more liquid mass. The calculations from which Figure 4 was obtained show an increase of δ with K_{p1}. This is the effect of the greater final temperature, not its cause. The break in the curve for $K_{p1} = .05$ is again due to the complete vaporization of all the particles.

The effect of the Mach number on T_3/T_1 is shown in Figure 5. The curves show that the final temperature increases with shock strength exactly as would be expected. They also show a greater tendency towards complete evaporation of the liquid in the stronger shocks. This is also to be expected, since the final equilibrium concentration increases with increasing final temperature. The same qualitative dependence of temperature on Mach number could also be seen in the case where $h_\ell/(RT_1)$ is such that condensation occurs.

It has been noted earlier that the final temperature is higher for lower values of $h_\ell/(RT_1)$, and that these cases correspond to greater vapor condensation. It can be seen from equation (4) that the change of K_{v3} with T_3 is positive. But if this is true, one would expect that higher final temperatures correspond to greater vapor evaporation. This apparent paradox can be resolved by considering the pressure ratio, p_3/p_1. Figure 6 is a typical plot of p_3/p_1 versus K_{v1} for several values of $h_\ell/(RT_1)$. The conditions are the same as for Figure 2. An explanation of the variation of p_3/p_1 with $h_\ell/(RT_1)$ will be postponed until after u_3/u_1 has been discussed. It can be seen immediately, though, that the final pressure is considerably greater

than the initial one. This has the result of reducing K_{v3} and countering the effect of the temperature rise. Unless the multiplier in the exponential term, $h_\ell/(RT_1)$, is sufficiently large, the importance of the temperature increase will be surpassed by the pressure rise and the equilibrium concentration will be reduced.

It is of considerable interest to note that both condensation and evaporation of the liquid particle may occur. Condensation occurs when the physical constants of the system are such that the pressure rise after the shock has a greater effect on the equilibrium concentration than the temperature rise after the shock. Another, more formal, way of saying this is as follows. In certain cases, the shape of the saturation curve, which is in part determined by $h_\ell/(RT_1)$, is such that state 3 is deeper inside the vapor dome than state 1.

The ratio of the final velocity to the initial velocity is shown plotted in Figures 7 and 8. Figure 7 is for the same condition as Figures 1, 2, and 6, and Figure 8 corresponds to the conditions of Figure 3.

The energy equation can be written as

$$\frac{\dot{w}}{\rho_1 u_1}(c_p T_3 + \tfrac{1}{2}u_3^2) + \delta h_\ell = \text{const},$$

where $\dot{w}$ is the total mass flow, $(\rho_3+\rho_{p3})u_3$. Thus, once the variation of T_3 and δ with K_{p1} and $h_\ell/(RT_1)$ has been determined, the changes in u_3 with these quantities are fixed by the conservation of energy. Having been able to explain and understand Figures 1, 2, and 3, the variation of u_3 with $h_\ell/(RT_1)$ and K_{p1} on Figures 7 and 8

is a consequence of these facts and the energy equation.

In a similar manner, but using the momentum equation, the variation of the curves in Figure 6 can be explained from Figure 7. The momentum equation can be written as

$$\frac{p_3}{p_1} + \frac{u_1 \dot{w}}{p_1} \frac{u_3}{u_1} = \text{const.}$$

Since the momentum at state 1 is the same for all the cases on Figure 6, the constant on the right hand side is the same. Denoting different values of $h_\ell/(RT_1)$ by superscripts, the above expression can be written as

$$\left[\left(\frac{p_3}{p_1}\right)^2 - \left(\frac{p_3}{p_1}\right)^1\right] = -\gamma M_1^2 (1+K_{p1}) \left[\left(\frac{u_3}{u_1}\right)^2 - \left(\frac{u_3}{u_1}\right)^1\right].$$

Thus, given Figure 7, the variation of p_3/p_1 with $h_\ell/(RT_1)$ on Figure 6 is fixed by the conservation of momentum.

VI. STRUCTURE OF THE EQUILIBRATION ZONE

The differential equations derived in Section II describe the one-dimensional motion of a mixture of liquid particles, its vapor, and a gas. If these equations are integrated from state 2, just downstream of the shock, to state 3, the details of the equilibration process will be known.

The conditions at state 2 can be found quite readily. It is generally accepted[1-4] that the particles are not affected by the shock itself. This is because the thickness of the shock is so much less than the velocity, temperature, and diffusion ranges of the particles. Hence, at state 2 the properties of the particles are the same as they were at state 1. Since the thickness of the shock is such that the particles are not affected by the gas as they travel through the shock, it must also be that the particles do not affect the fluid. Thus, the changes in fluid properties are given by the conventional shock relations.

$$\frac{u_2}{u_1} = \frac{2}{(\gamma+1)M_1^2}\left(1 + \frac{\gamma-1}{2} M_1^2\right)$$

$$\frac{p_2}{p_1} = 1 + \frac{2\gamma}{\gamma+1}\left(M_1^2 - 1\right)$$

$$\frac{T_2}{T_1} = \left[1 + \frac{2\gamma}{\gamma+1}\left(M_1^2-1\right)\right]\left[1 - \frac{2}{\gamma+1}\frac{M_1^2-1}{M_1^2}\right]$$

Formulation of the Mathematical Problem

The structure of the equilibration zone, from state 2 to state 3, involves three differential equations, equations (18), (19), and (20). Inspection of these equations shows that the independent variable x is

not essential to the problem and that it can be eliminated quite easily. The role of independent variables can be delegated to any of the other variables. The particle velocity, u_p, was chosen for this position. Dividing equations (18) and (20) by (19) eliminates the coordinate x and reduces the number of equations by one. The results are

$$c\frac{dT_p}{du_p} = c\frac{\lambda_{v_3}}{\lambda_{T_3}}\frac{1+\frac{\lambda_{T_3}}{\lambda_{D_3}}(K_v-K_v^e)}{1+\frac{\lambda_{v_3}}{\lambda_{D_3}}(K_v-K_v^e)}\frac{T_p-T}{u_p-u} - h_\ell\frac{\lambda_{v_3}}{\lambda_{D_3}}\frac{K_v-K_v^e}{[1+\frac{\lambda_{v_3}}{\lambda_{D_3}}(K_v-K_v^e)](u_p-u)} \tag{26}$$

and

$$\frac{dK_v}{du_p} = \frac{\lambda_{v_3}}{\lambda_{D_3}}\frac{1-K_v}{1-K_{v3}}\frac{K_{p3}(1-K_v)-(K_v-K_{v3})}{1+\frac{\lambda_{v_3}}{\lambda_{D_3}}(K_v-K_v^e)}\frac{K_v-K_v^e}{u_p-u} \quad . \tag{27}$$

These are now two equations in four unknowns; T_p, T, u, and K_v. However, equation (27) involves only K_v and u. Therefore, by eliminating T and T_p from equation (26), a system of two first-order non-linear equations in two unknown results. The elimination of T and T_p can be accomplished by utilizing the overall momentum and energy equations, equations (5) and (6). Upon doing this, there results

$$\frac{\gamma}{\gamma-1}\left[\frac{\gamma+1}{\gamma}u(\rho u)+(\rho_p u_p)u_p - M_o\right]\frac{du}{du_p} = (\rho_p u_p)\left[u_p - \frac{\gamma}{\gamma-1}u - \frac{\lambda_{v_3}}{\lambda_{D_3}}\right.$$

$$\left.\frac{h_\ell}{1+\frac{\lambda_{v_3}}{\lambda_{D_3}}(K_v-K_v^e)}\frac{K_v-K_v^e}{u_p-u}\right]+\frac{\lambda_{v_3}}{\lambda_{T_3}}\frac{1+\frac{\lambda_{T_3}}{\lambda_{D_3}}(K_v-K_v^e)}{1+\frac{\lambda_{v_3}}{\lambda_{D_3}}(K_v-K_v^e)}\frac{1}{u_p-u}\left\{(\rho_3 u_3-\rho u)h_\ell+\frac{\gamma}{\gamma-1}p_3\right.$$

$$\left.[(1+K_{p3})u_3-u-K_p u_p]+\tfrac{1}{2}[\dot{w}u_3^2-(\rho u)u^2-(\rho_p u_p)u_p^2]-\frac{\gamma}{\gamma-1}\frac{\dot{w}u}{\rho u}[\dot{w}u_3-(\rho u)u-\right.$$

$$\left.(\rho_p u_p)u_p]\right\}-\frac{1}{\rho_p u_p}\left\{\dot{w}h_\ell-\frac{\gamma+1}{2(\gamma-1)}\dot{w}u^2+\frac{\gamma}{\gamma-1}M_o u-E\right\}\frac{d(\rho_p u_p)}{du_p} \quad , \tag{28}$$

where E is the total energy flux and M_o is the left hand side of the momentum equation, equation (5). ρu, $\rho_p u_p$, K_p, and $\frac{d(\rho_p u_p)}{du_p}$ have been left in simply for convenience in writing; they could be eliminated in terms of K_v by use of equations (2) and (3).

Throughout this discussion, K_v^e has been regarded as a known function of u_p. This, of course, is not true. K_v^e depends on p and T_p, as given by equation (4). But in order to have T_p and p as known functions of u_p, the momentum and energy equations must be solved. In order to solve these, the two continuity equations, (2) and (3), must also be solved. Thus, the problem is really not just one of integrating two simultaneous differential equations, but one of simultaneously solving five algebraic equations and integrating two differential ones. Due to the obvious complexities, a Runge-Kutta formula for a numerical solution was used. The method and program were both routine enough so their documentation was not warranted. The results of these calculations for three sets of initial conditions are shown in Figures 9 through 20. The figures will be discussed later.

Equations (19) can be rearranged to

$$\frac{x}{\lambda_{v3}} = \int_{u_1}^{u_p} \frac{u_p \Sigma du_p}{a(u_p - u)\left[1 + \frac{\lambda_{v3}}{\lambda_{D_3}}(K_v - K_v^e)\right]} \quad . \tag{29}$$

Hence, once the differential equations (27) and (28) have been integrated so that all of the state variables are known as functions of u_p, x/λ_{v3} can be found as a function of u_p from the above quadrature.

Singularity Near the Equilibrium Point

Inspection of equations (26) and (27) reveals the fact that the point corresponding to state 3 is a singular point. This was to be expected since state 3 is an equilibrium state, and changes with respect to x of the particle variables should be zero. Indeed, this is exactly what equations (18) through (20) tell us. Thus, when two of these equations are divided by the third, the result should be zero over zero at equilibrium. This indeterminate form could cause serious computational difficulty when the stepwise numerical integration gets close to the final point. There are two ways out of this dilemma. One is to ignore the problem completely; since the final point of the solution is already known, the calculated points would be disregarded as soon as they started leading off in another direction. The other way out is to use a perturbation technique around the singularity to determine the limiting slope there. The latter approach was chosen as providing more information.

Expanding the fluid and particle properties in a Taylor series about state 3 gives

$$u = u_3 + \epsilon(u-u_3) + \ldots$$

$$u_p = u_3 + \epsilon(u_p-u_3) + \ldots$$

$$T = T_3 + \epsilon(T-T_3) + \ldots$$

$$T_p = T_3 + \epsilon(T_p-T_3) + \ldots$$

etc.

Introducing these equations into equation (1) gives to the first order

$$u_3(\rho-\rho_3) + \rho_3(u-u_3) + u_3(\rho_p-\rho_{p3}) + \rho_{p3}(u_p-u_3) = 0 \ .$$

The first order momentum equation is

$$\rho_3 u_3(u-u_3) + \rho_{p3} u_3(u_p-u_3) + p - p_3 = 0 ,$$

and the energy equation becomes

$$\frac{p_3 u_3}{1-K_{v3}}(K_v-K_{v3})h_\ell + \rho_3 u_3[c_p(T-T_3)+u_3(u-u_3)] + \rho_{p3} u_3[c_p(T_p-T_3) + u_3(u_p-u_3)] = 0 .$$

Also, to first order, the difference between the equilibrium concentration and the concentration at point 3 can be written as

$$\frac{K_v^e-K_{v3}}{K_{v3}} = \frac{h_\ell}{RT_3}\frac{T_p-T_3}{T_3} - \frac{p-p_3}{p_3} .$$

Near state 3, the two differential equations, (26) and (27), can be written as

$$\frac{d\left(\frac{T_p-T_3}{T_3}\right)}{d\left(\frac{u_p-u_3}{u_3}\right)} = \frac{\lambda_v}{\lambda_T}\frac{\left(\frac{T_p-T_3}{T_3}\right)-\left(\frac{T-T_3}{T_3}\right)}{\left(\frac{u_p-u_3}{u_3}\right)-\left(\frac{u-u_3}{u_3}\right)} - \frac{\gamma-1}{\gamma}\frac{h_\ell}{RT_3}\frac{\lambda_v}{\lambda_D}\frac{(K_v-K_v^3)-(K_v^e-K_v^3)}{\left(\frac{u_p-u_3}{u_3}\right)-\left(\frac{u-u_3}{u_3}\right)}$$

and

$$\frac{d(K_v-K_{v3})}{d\left(\frac{u_p-u_3}{u_3}\right)} = \frac{\lambda_{v3}}{\lambda_{D3}} K_{p3}(1-K_{v3}) \frac{(K_v-K_{v3})-(K_v^e-K_v^3)}{\frac{u_p-u_3}{u_3}-\frac{u-u_3}{u_3}}$$

where $\frac{\lambda_v}{\lambda_D}(K_v-K_v^e)$ and $\frac{\lambda_T}{\lambda_D}(K_v-K_v^e)$ have been neglected compared to 1. Since the perturbation is only valid near state 3, the differentials can be replaced by differences. The way the variables are written, the differences can in turn be written as the variables themselves, because they all vanish at state 3. The result is two algebraic equations.

Using the linearized continuity, momentum, and energy equations and the expression for $K_v^e - K_{v3}$ to eliminate all the unknowns except u and K_v, there results

$$H\left(\frac{\Delta u}{\Delta u_p}\right)^3 + (C+F+EH)\left(\frac{\Delta u}{\Delta u_p}\right)^2 + (A+D-C+EF+G)\frac{\Delta u}{\Delta u_p} + EG-A+B = 0 \quad (30)$$

and

$$\frac{\Delta K_v}{\Delta u_p} = \frac{\alpha K_{v3}[\delta + \omega + (\gamma' + 1 - \epsilon)(\Delta u/\Delta u_p)]}{(\alpha - \alpha\beta K_{v3} - 1) + (\Delta u/\Delta u_p)} \quad , \quad (31)$$

where

$$\Delta u_p = \frac{u_p - u_3}{u_3}$$

$$\Delta u = \frac{u - u_3}{u_3}$$

$$\Delta K_v = K_v - K_{v3}$$

$$\alpha = \frac{\lambda_v}{\lambda_D} K_{p3}(1 - K_{v3})$$

$$\beta = \frac{\lambda_v}{\lambda_D} \frac{h_\ell/(RT_3)}{\alpha}\left(1 - \frac{\gamma-1}{\gamma}\frac{h_\ell}{RT_3}\right)$$

$$\gamma' = \frac{h_\ell}{RT_3}\frac{1}{K_{p3}}(M_3^2 - 1)$$

$$\delta = \frac{h_\ell}{RT_3} M_3^2$$

$$\epsilon = 1 - \gamma M_3^2$$

$$\omega = \gamma K_{p3} M_3^2$$

$$A = \frac{\lambda_v}{\lambda_D}\gamma K_{v3} M_3^2 \left(\frac{h_\ell}{a_3^2} + K_{p3}\right)$$

$$B = \frac{\lambda_v}{\lambda_T} A\left[1 + K_{p3} - (\gamma-1)\frac{h_\ell}{a_3^2}\right]$$

$$C = \frac{\lambda_v}{\lambda_D} \gamma K_{v3} \left[M_3^2 + \frac{h_\ell}{a_3^2 K_{p3}} (M_3^2 - 1) \right]$$

$$D = BC/A$$

$$E = \frac{\lambda_v}{\lambda_D} K_{p3} (1 - K_{v3}) - \frac{\lambda_v}{\lambda_D} \gamma K_{v3} \frac{h_\ell}{a_3^2} \left[1 - (\gamma - 1) \frac{h_\ell}{a_3^2} \right] - 1$$

$$F = \frac{(\lambda_v/\lambda_T) - 1}{K_{p3}} (M_3^2 - 1) + M_3^2 \left(\frac{\lambda_v}{\lambda_T} \gamma - 1 \right) - \frac{\lambda_v}{\lambda_T}$$

$$G = M_3^2 \left(\frac{\lambda_v}{\lambda_T} - 1 \right) + \frac{\lambda_v}{\lambda_T} \gamma K_{p3} M_3^2$$

$$H = (M_3^2 - 1)/K_{p3}$$

It can be seen that equation (30) is a cubic and therefore has three roots. In calculating some examples, it was found that all three roots were real. There was no difficulty in deciding which root was relevant, though; the numerical integration proceeded far enough without difficulty so the choice was a clear one.

Numerical Calculations

Three sets of calculations were made to illustrate the three different cases possible; δ less than one, greater than one, and complete vaporization of all the liquid at equilibrium. A description of the results will make the equilibration process clear.

Figures 9 through 13 show the outcome of the first set of calculations. The initial conditions are $M_1 = 1.6$, $K_{v1} = .2$, $K_{p1} = .1$, and $h_\ell/(RT_1) = 10$. δ is approximately 1.08. The first figure of the group shows u plotted against u_p. Both of these quantities are non-dimensionalized by division by their equilibrium value, u_3. This is also true of all the other variables in all the other figures except

for K_v. u_p was chosen as the independent variable in this and the other figures simply because it was used in that role in the calculations. The straight dashed line in the figure is the final slope as calculated from equation (30). It has the value .98. Thus, it can be seen that when u_p/u_3 is less than about 1.1, the particles and fluid are essentially travelling at the same speed. The hatch marks along the curve represent the results of equation (29). The figure shows that the distance in which the velocities equalize is rather short. Theoretically, it takes an infinite distance for the system to reach full equilibrium. The calculations were not carried close enough to the singularity to determine the location of larger values of x/λ_{v3}. If this were done, it would show that the distance in which the velocity equalized is followed by a much longer one in which the other properties attain their equilibrium values.

Discussion of the Results

The effect of vapor evaporation is very small in the initial period. This is shown in two ways. First, a quantity u^*/u_3 has been calculated and its value is indicated on the coordinate in Figure 9. This is the ratio of the final velocity for solid particles to the final velocity in this case. It is seen that the curve heads toward this point until, at low values of u_p/u_3, it changes direction. Further proof that initially the vaporization is not important can be seen clearly from Figure 10. This is a plot of $K_v - K_{v3}$ against u_p/u_3. Again, the dotted line indicates the limiting slope, which is -.909. It can be seen that there is almost no change in the concentration

down to a value of 1.4 for u_p/u_3, and very little down to values of 1.2 or even 1.1. Then, after the particles have almost reached their final velocity and the relative speed between the fluid and particles is almost zero, most of the vaporization takes place. K_v is the ratio of two quantities, both of which are changing. In order to avoid the ambiguity caused by this, Figure 11 is a graph of $(\rho_p u_p)/(\rho_3 u_3)$ plotted against u_p/u_3. This clearly shows little change in particle mass flow rate until u_p/u_3 is close to unity.

Both Figures 10 and 11 show that for values of u_p/u_3 greater than about 2.15, there is condensation of the vapor on the particles. This can be observed from the fact that K_v is decreasing when the curve is read from right to left, the direction in which the process is proceeding. On Figure 11 the same thing is shown by the increase in particle mass flow rate initially. This is caused by the sudden change in the equilibrium constant across the shock. On the downstream side of the shock, the particle temperature is still very nearly T_1, but the fluid pressure has risen sharply. This causes the equilibrium concentration to decrease while the actual concentration is still K_{v1}. Thus, the condition exists in which the concentration is larger than the equilibrium concentration and vapor is forced to condense. This always occurs.

The fluid and particle temperatures are shown in Figure 12. The particle temperature rises rapidly near the shock and then heads toward T_3 almost linearly with u_p. The fluid temperature is fairly constant near the shock, but heading toward T^*/T_3, where T^* is the value of T_3 if the particles were non-volatile. Then, as the evapora-

tion process becomes the dominant phenomenon, the temperature falls off rapidly to T_3 . It appears that at first the condensation of vapor and heat transfer from the fluid combine to quickly raise the particle temperature. Meanwhile, the heat lost by the fluid has been replaced by conversion of kinetic energy. Finally, when the majority of evaporation takes place, all of the necessary latent heat is supplied by the fluid.

The next set of figures, 13 through 16, illustrates what the curves look like when δ is less than one. Figure 13, which shows u/u_3 plotted against u_p/u_3 , is very similar to Figure 9. There are some differences, though. The curve approaches its final slope, .82, in a much shorter distance in terms of x/λ_{v3} than did the curve in Figure 9. This is primarily caused by the difference in λ_{v3} due to Σ being less than one for this figure and greater than one for Figure 9. The tendency to head for u^*/u_3 is not as obvious from this case as the previous one.

The tendency for the vapor concentration to exceed the equilibrium concentration immediately downstream of the shock has been explained above. The difference in the two cases, however, is that this tendency is not reversed in the present instance, while it was for the one before. This is illustrated in Figure 14, which is a plot of $K_v - K_{v3}$ against u_p/u_3 . Here, the concentration starts decreasing initially and continues to decrease, but with a much greater rate for small values of u_p/u_3 . Again, it should be noted that the slope is quite small for most values of u_p/u_3 , indicating there is little condensation until the two velocities have almost equalized. The same

thing is shown in Figure 15, which is a plot of $(\rho_p u_p)/(\rho_3 u_3)$.

Somewhat different results than were obtained before are shown in Figure 16. This figure shows the variation of T_p/T_3 and T/T_3 with u_p/u_3. As in Figure 12, T_p/T_3 starts rising rapidly as soon as the shock is crossed, but now it continues this rise all the way to T_3. T behaves much the same way it did before, but now the fluid temperature is increased rather than decreased while the major portion of the change of phase is going on. Obviously, this is due to the fact that vapor is being condensed. At large values of u_p/u_3, when the temperature difference between the fluid and particles is large, Figures 14 and 15 show that the amount of vaporization is small. It is the sum of those two effects, heat transfer and heat addition from vaporization, which accounts for the particle temperature rise. At moderate values of u_p/u_3 the temperature difference is not nearly as large, but now the amount of condensation has increased, providing about the same total amount of heat to the particles as before. The increasing rate of condensation continues to provide enough heat for the particle temperature to rise even after the particles are hotter than the fluid. Finally, so much heat is given off that it strongly affects the fluid temperature.

The final calculations were for the case where no particles remain at state 3. The conditions correspond to the point $K_{v1} = .2$ on the $h_\ell/(RT_1) = 10$ curve of Figure 3. This is well into the superheated region.

Figures 17, 18, and 19 are very similar to their counterparts from the first set of calculations, the other one involving

eventual vapor evaporation. There are some differences between Figures 12 and 20 which will be explained later.

Neither the limiting slope nor the value of x/λ_{v3} is shown in Figure 17. The case is special enough to invalidate the equations used to calculate those quantities. In deriving equations (30) and (31), the terms $K_v - K_{v3}$ and $K_v^e - K_{v3}$ were assumed to be of the same order. In this case they are not. Actually, inspection of the differential equations yields the result that both slopes should be infinite at the origin. The reason why equation (29) cannot be used is that λ_{v3} is zero.

Because of the model chosen, state 3 is reached as soon as all the particles have been evaporated. This must be; when the particles are gone, there is nothing left to be out of equilibrium with the fluid. It was expected that this phenomenon could be shown more clearly than it is. The fact that the velocities nearly equalize before the major portion of the evaporation takes place hides this. Only Figure 20 illustrates the phenomenon. For values of u_p/u_3 greater than 1.2, the figure is very similar to Figure 12. However, on Figure 20, the slow linear climb to T_3 is interrupted by the evaporation process. This is why the temperature climbs so steeply for u_p/u_3 less than about 1.1.

REFERENCES

1. Carrier, G. F., "Shock Waves in a Dusty Gas, J. Fluid Mech. 4 (1958).

2. Marble, Frank E., "Dynamics of a Gas Containing Small Solid Particles," Combustion and Propulsion (5th AGARDograph Colloquium), Pergamon Press (1963).

3. Rudinger, G., "Some Properties of Shock Relaxation in Gas Flows Carrying Small Particles," Physics of Fluids, Part I, Vol. 7 (May 1964).

4. Kriebel, A. R., "Analysis of Normal Shock Waves in Particle Laden Gas," J. Basic Eng., Trans. ASME, Series D, Vol. 86 (1964).

NOMENCLATURE

A_s	surface area of particle
a	local speed of sound
c	specific heat of liquid in particles
c_p	specific heat at constant pressure
D	diffusion coefficient
F	force
h	heat transfer coefficient
h_D	mass transfer coefficient
h_ℓ	heat of vaporization of liquid
K	concentration of vapor or particles in mixture, $\rho_v/(\rho_v+\rho_g)$ or $\rho_p(\rho_v+\rho_g)$
k	thermal conductivity
M	local Mach number
m	mass of single particle
$\dot{m}$	rate of mass vaporized from each particle
n	number of particles per unit volume
p	fluid pressure
R	gas constant
T	fluid temperature
u	velocity
v	specific volume
w	rate of mass given off by all the particles per unit volume
x	Cartesian coordinate
γ	ratio of specific heats

δ	ratio of mass rate of flow of fluid at state 3 to that at state 1
λ	characteristic length for equilibration of particles
μ	fluid viscosity
ρ	fluid density
Σ	$(\sigma/\sigma_3)^2$
τ	characteristic time for equilibration of particle

Subscripts

1	condition upstream of shock
2	condition immediately downstream of shock
3	equilibrium condition far downstream of shock
p	particle
v	vapor
g	gas
ℓ	liquid
T	temperature
D	diffusion

Superscripts

e	equilibrium

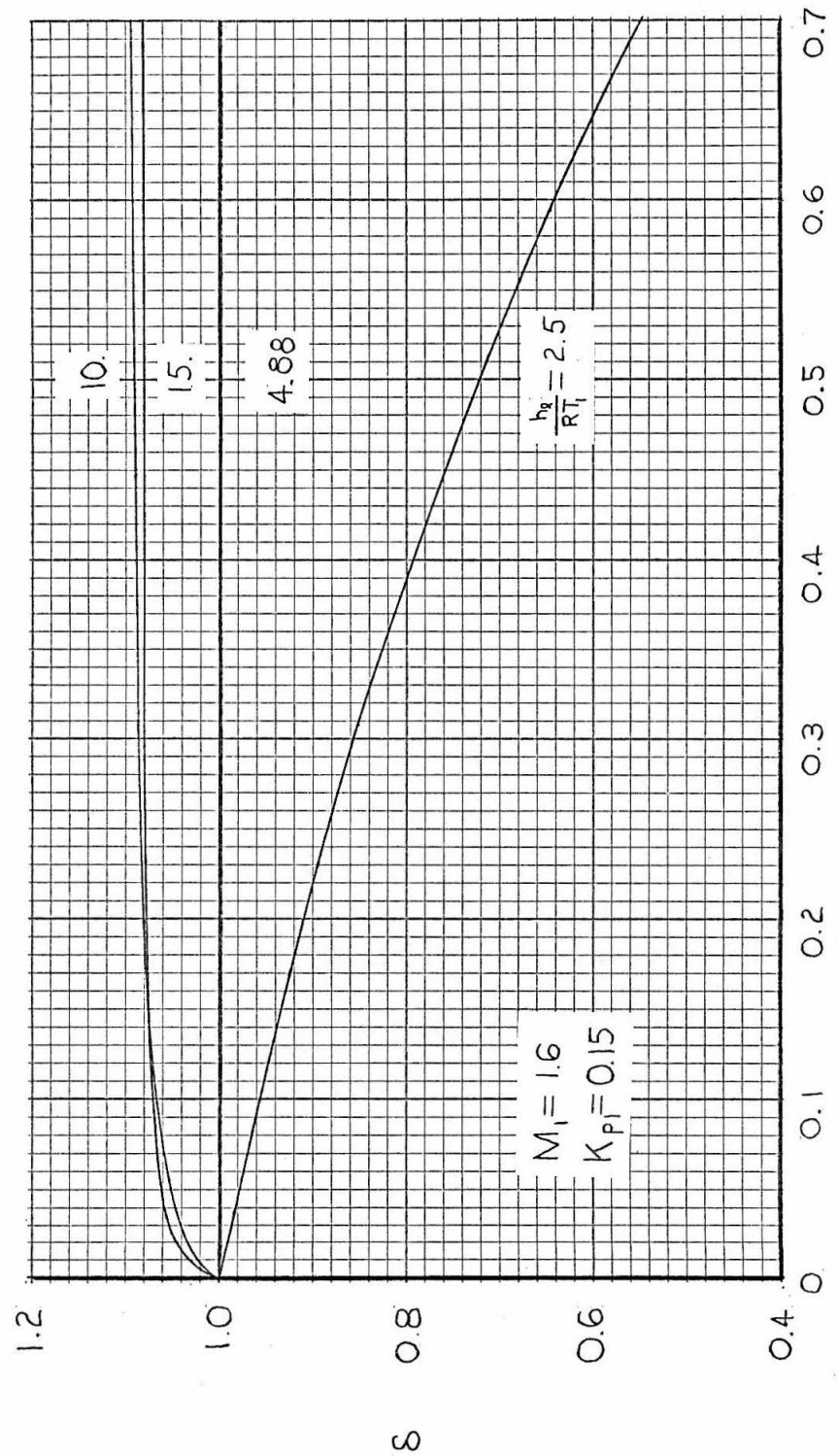

Figure 1. Dependence of δ on K_{v1} and $h_2/(RT_1)$.

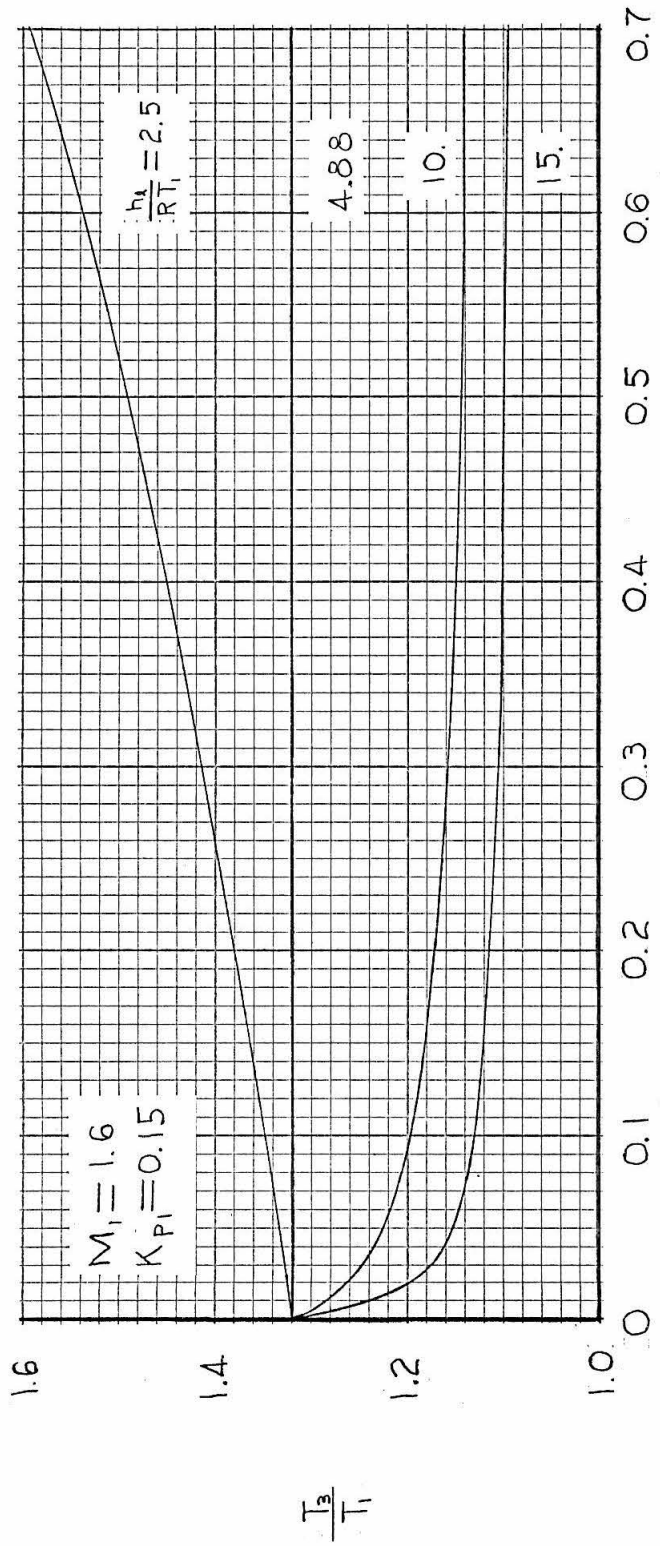

Figure 2. Variation of T_3/T_1 with K_{v1} and $h_\ell/(RT_1)$ at $K_{p1} = .15$.

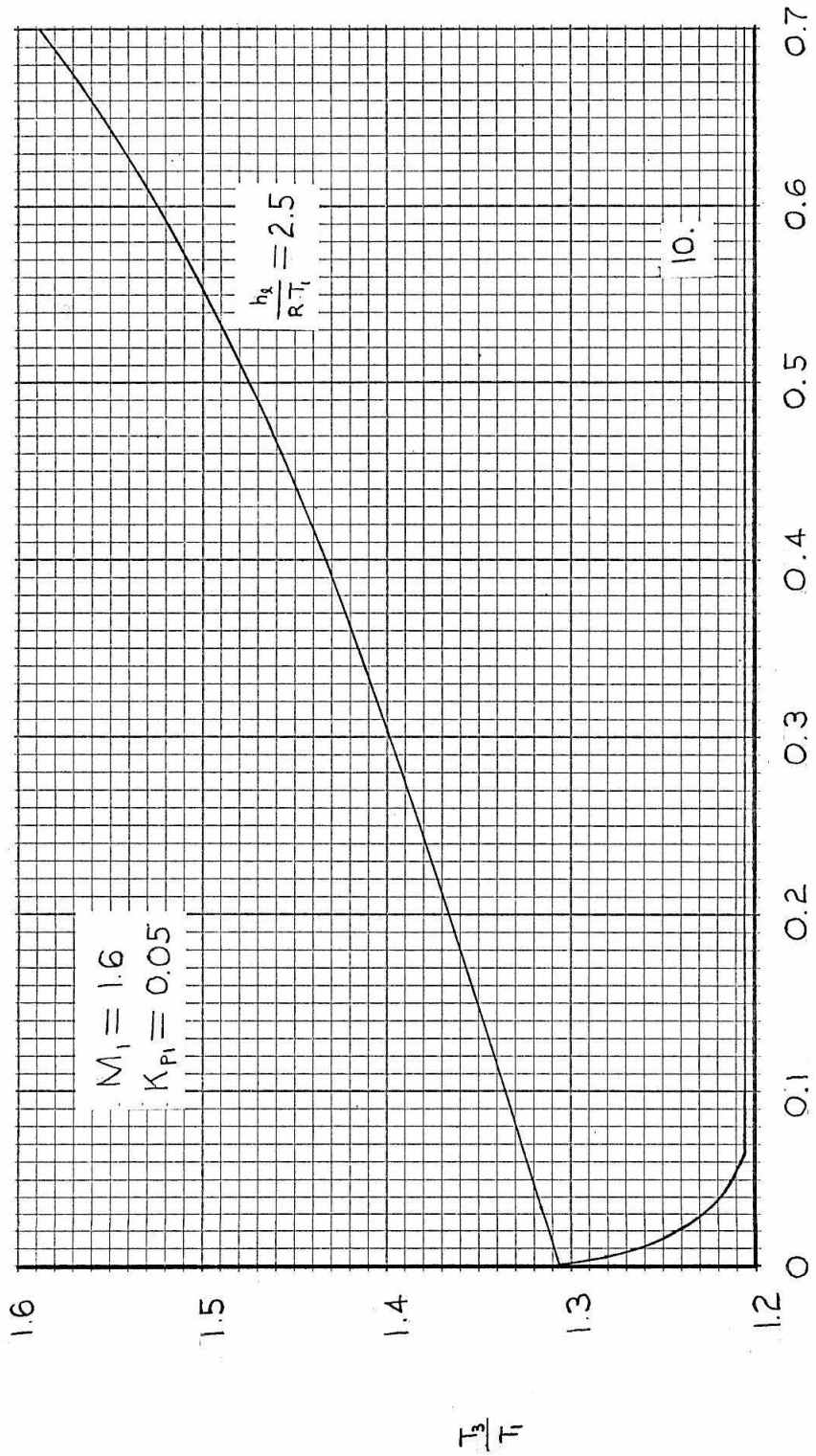

Figure 3. Variation of T_3/T_1 with K_{v1} and $h_\ell(RT_1)$at $K_{p1} = .05$.

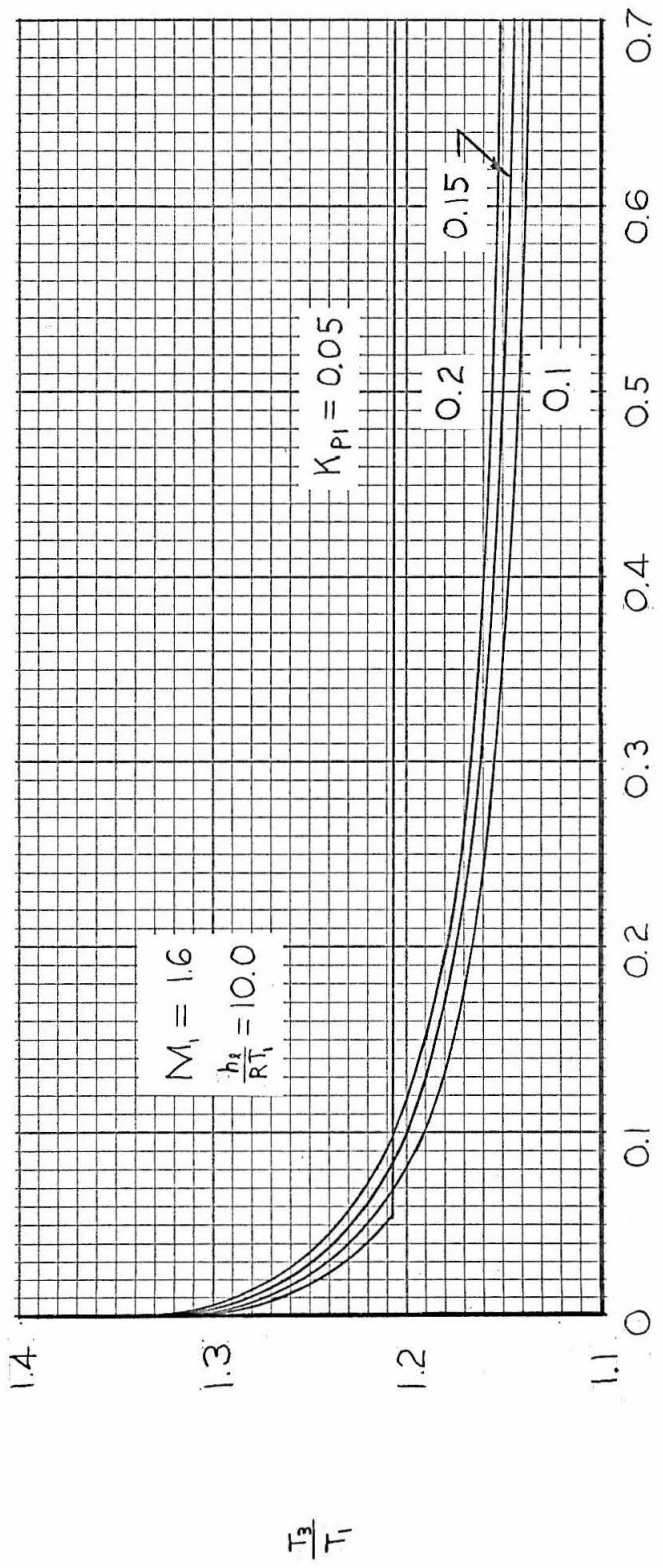

Figure 4. Variation of T_3/T_1 with K_{v1} and K_{p1}.

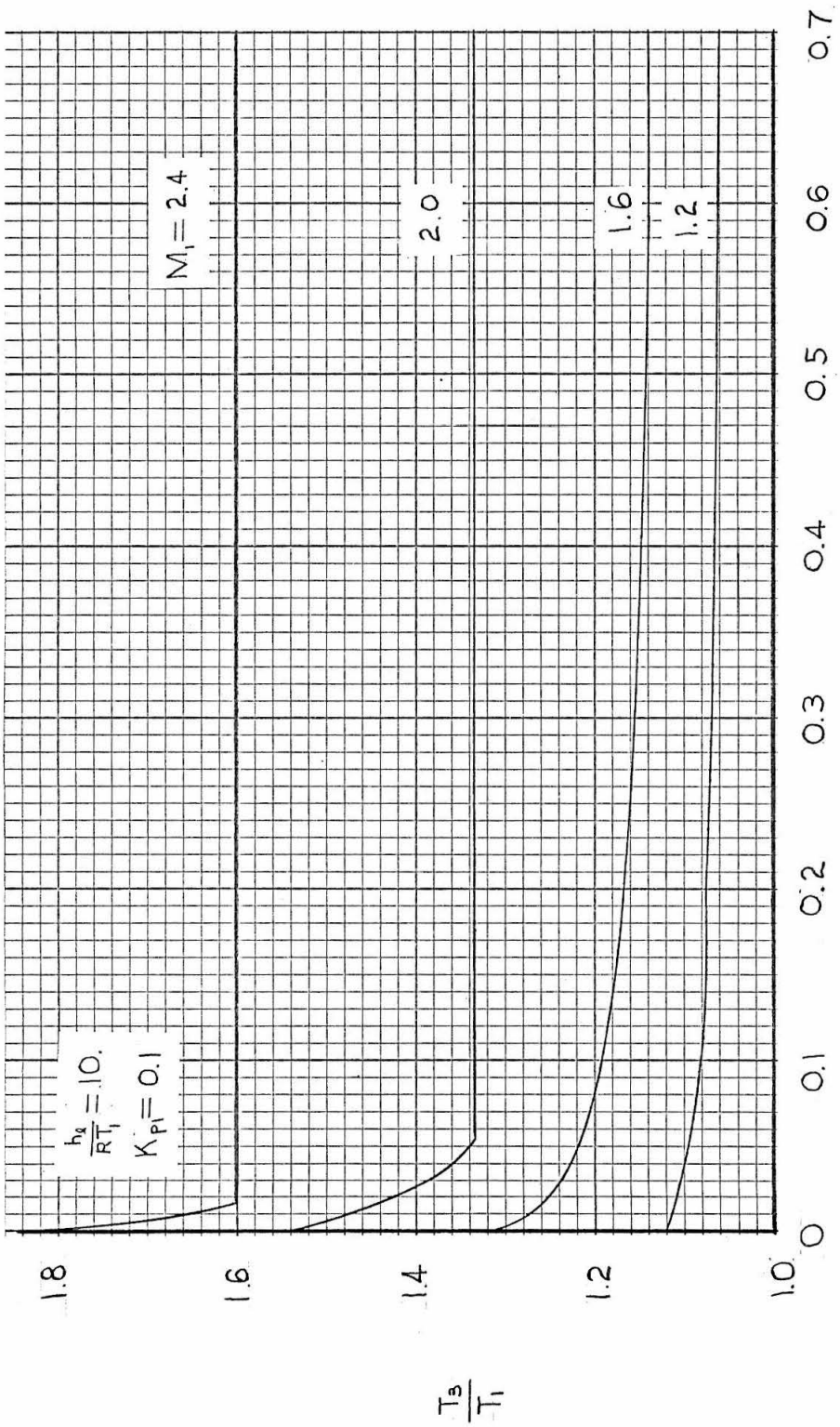

Figure 5. Variation of T_3/T_1 with K_{v1} and M_1.

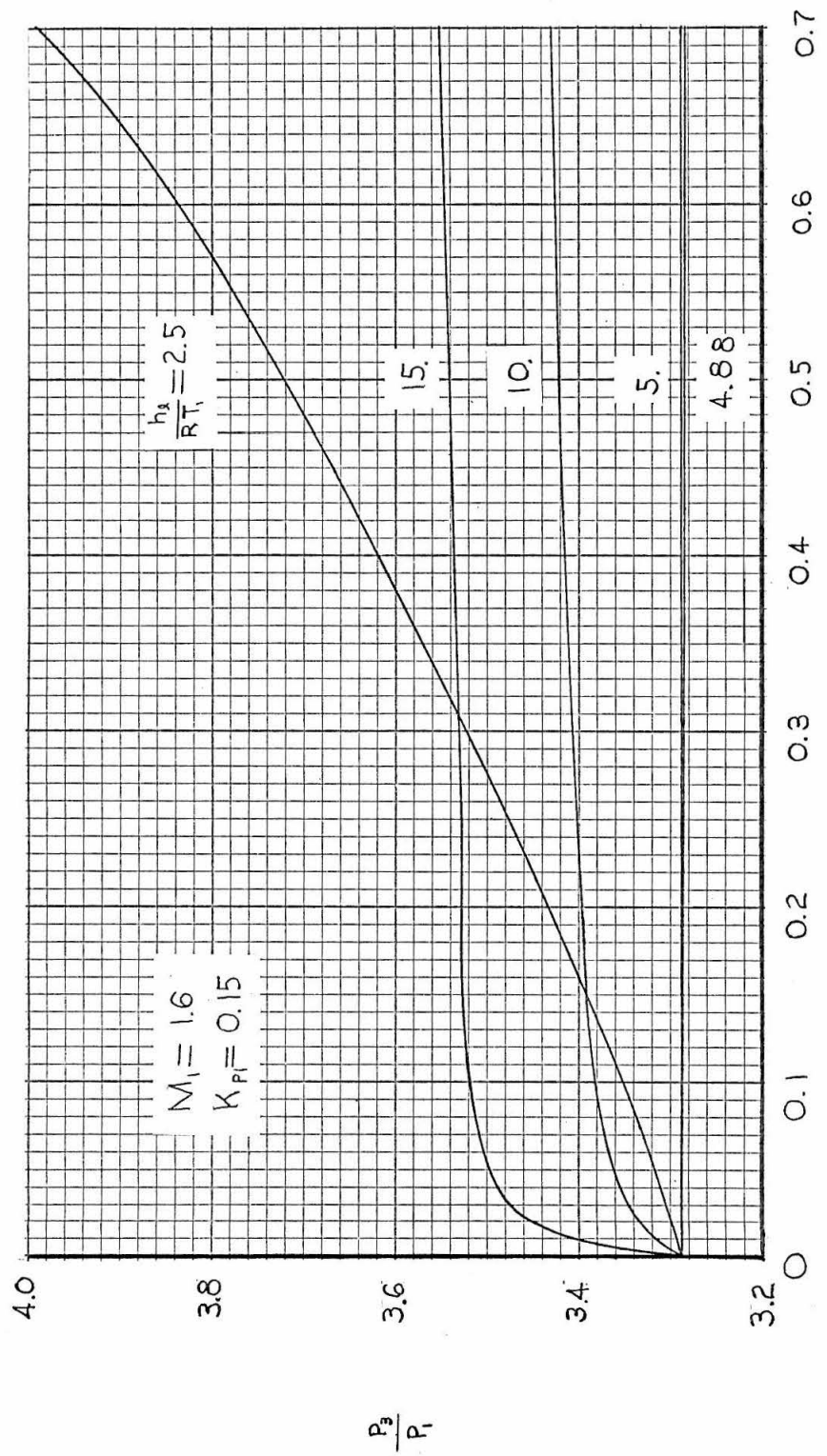

Figure 6. Typical Dependence of p_3/p_1 on K_{v1} and $h_\ell/(RT_1)$.

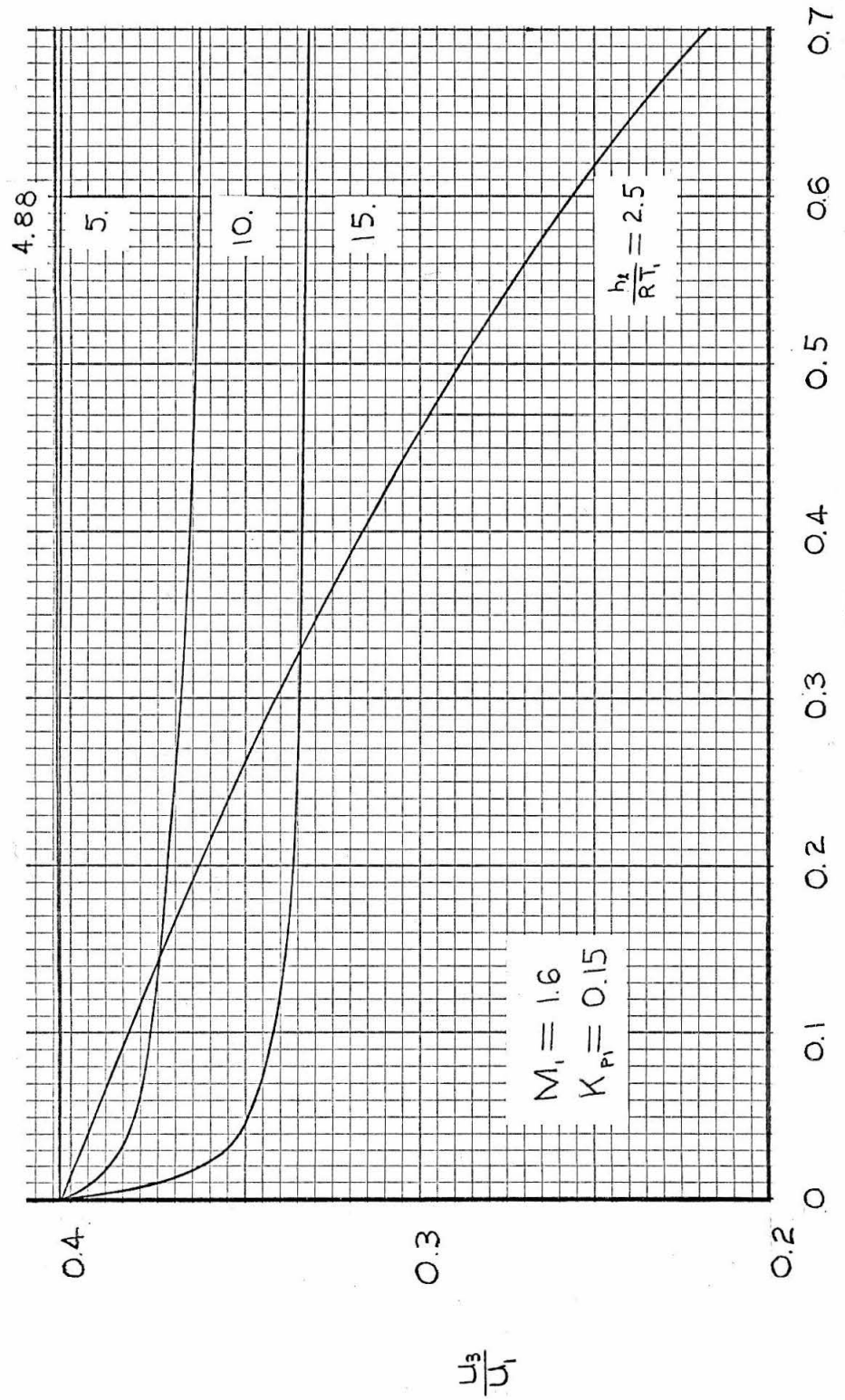

Figure 7. Variation of u_3/u_1 for Conditions of Figure 2.

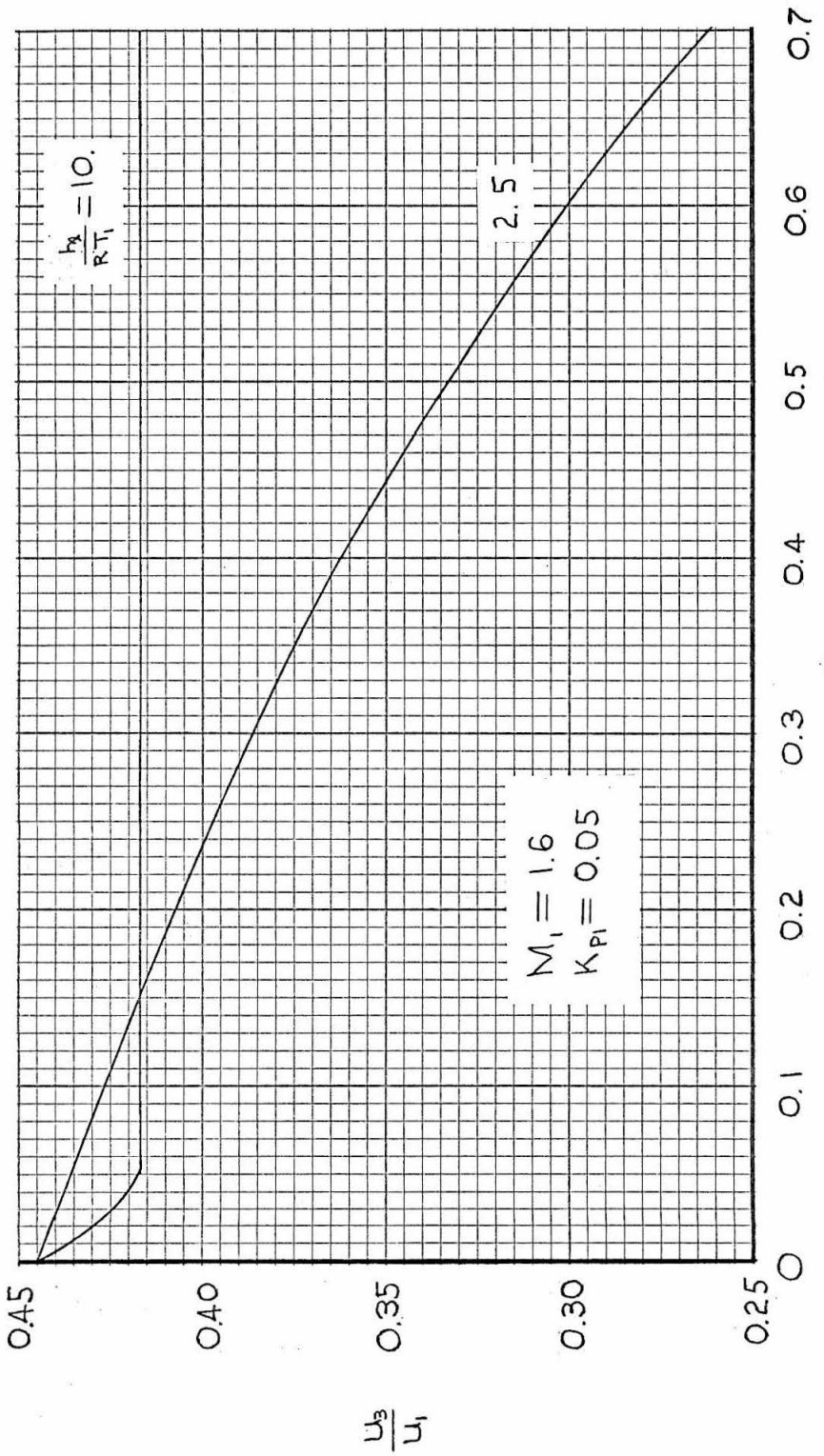

Figure 8. Variation of u_3/u_1 for Conditions of Figure 3.

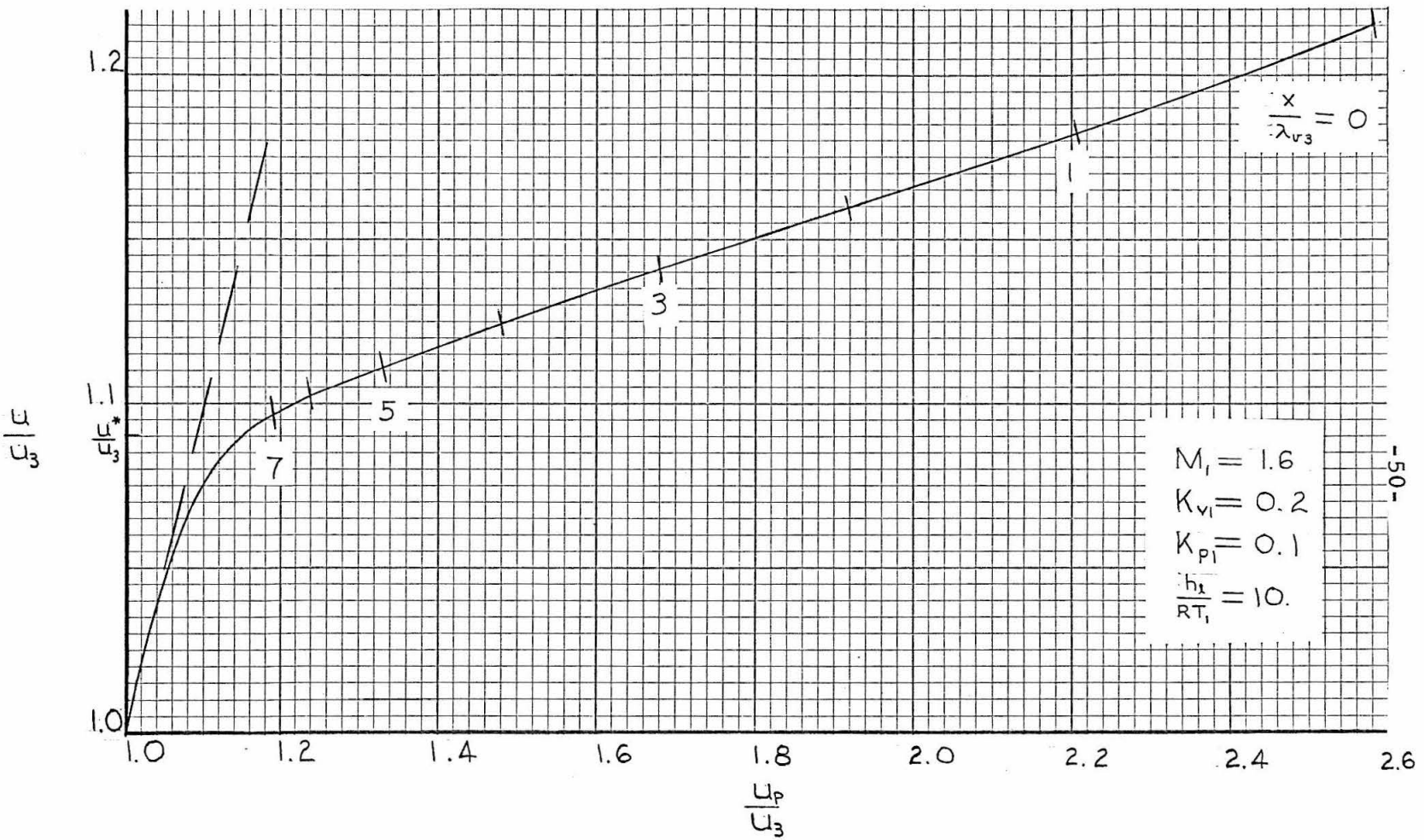

Figure 9. Velocity Equilibration for a Typical Case with $\delta > 1.0$.

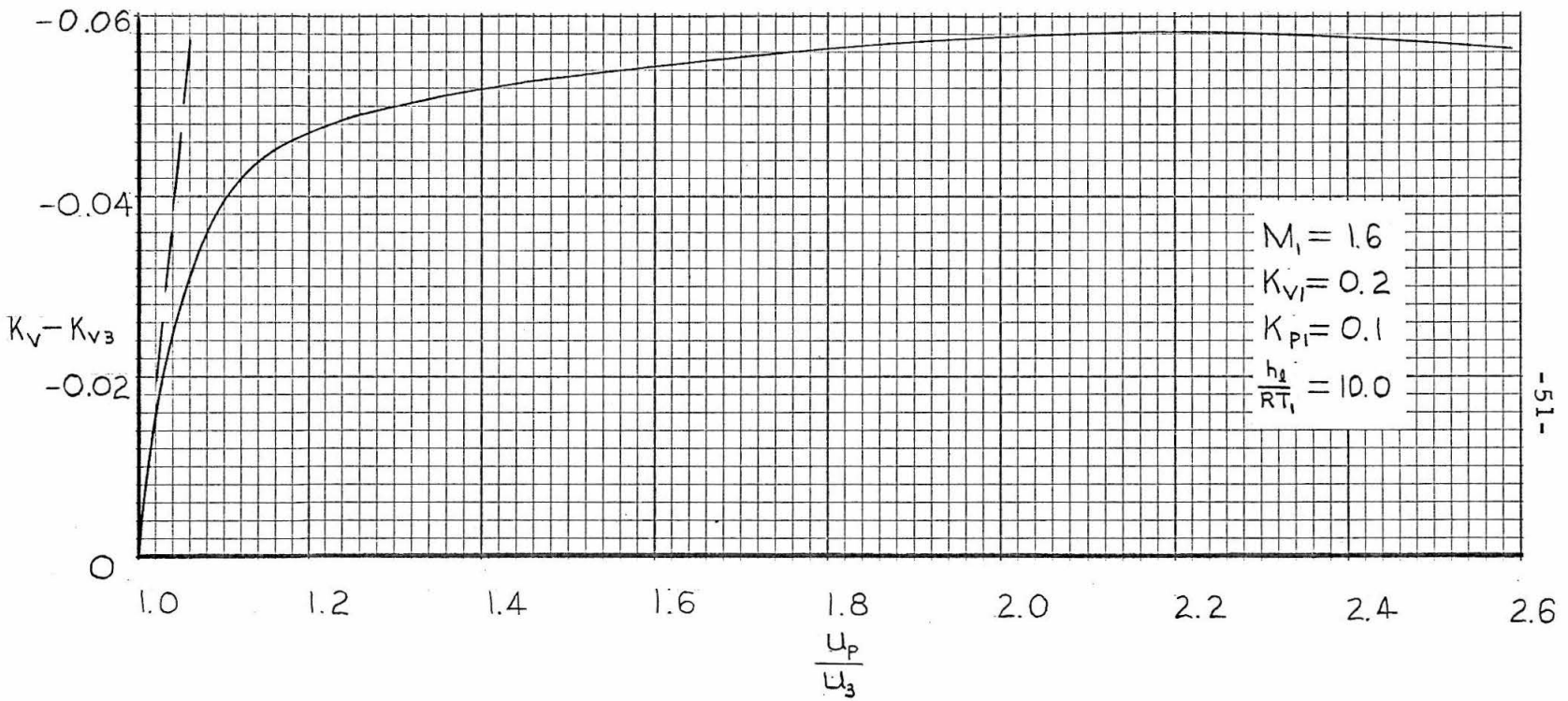

Figure 10. Vapor Concentration Equilibration for a Typical Case with $\delta > 1.0$.

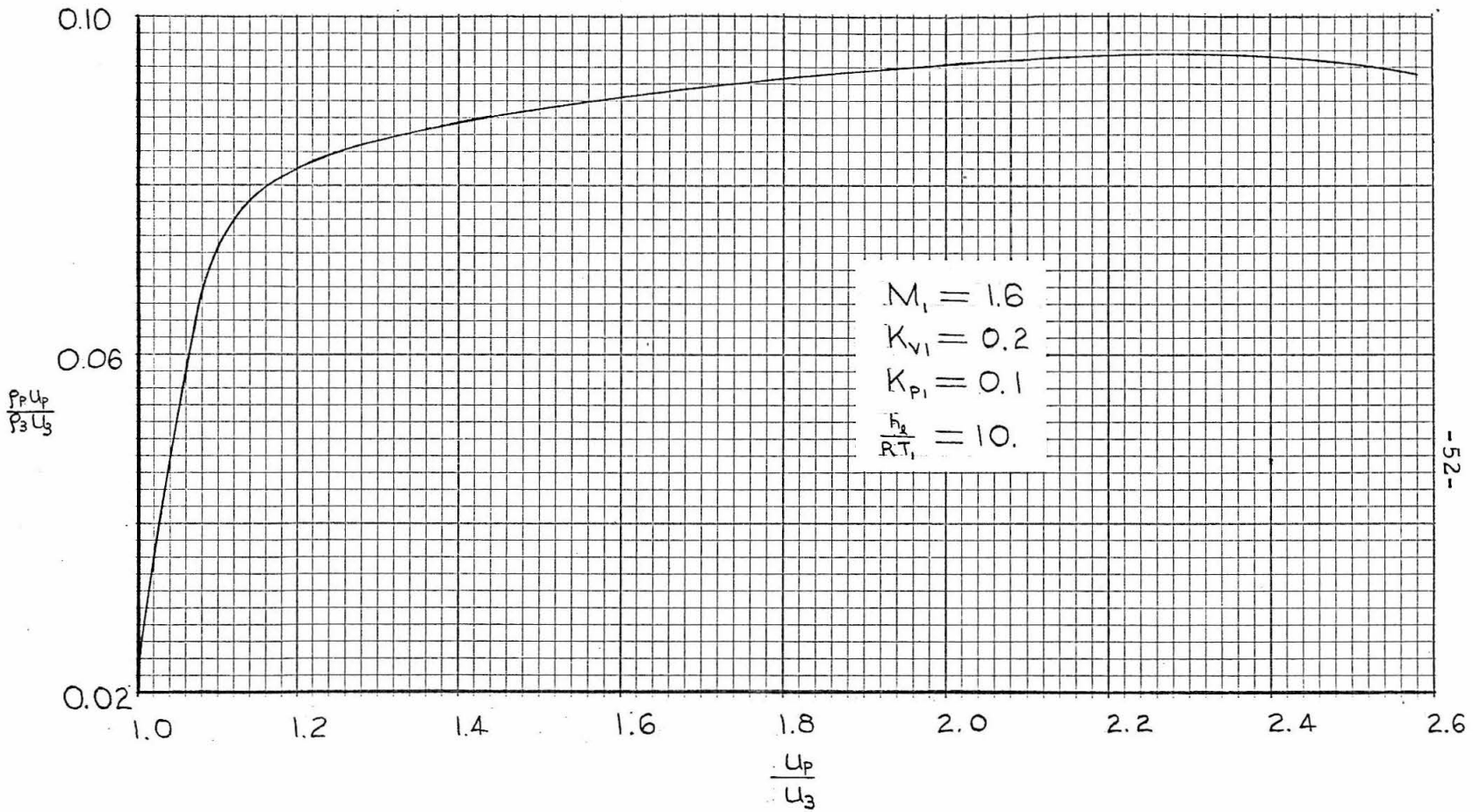

Figure 11. Particle Mass Flow Equilibration for a Typical Case with $\delta > 1.0$.

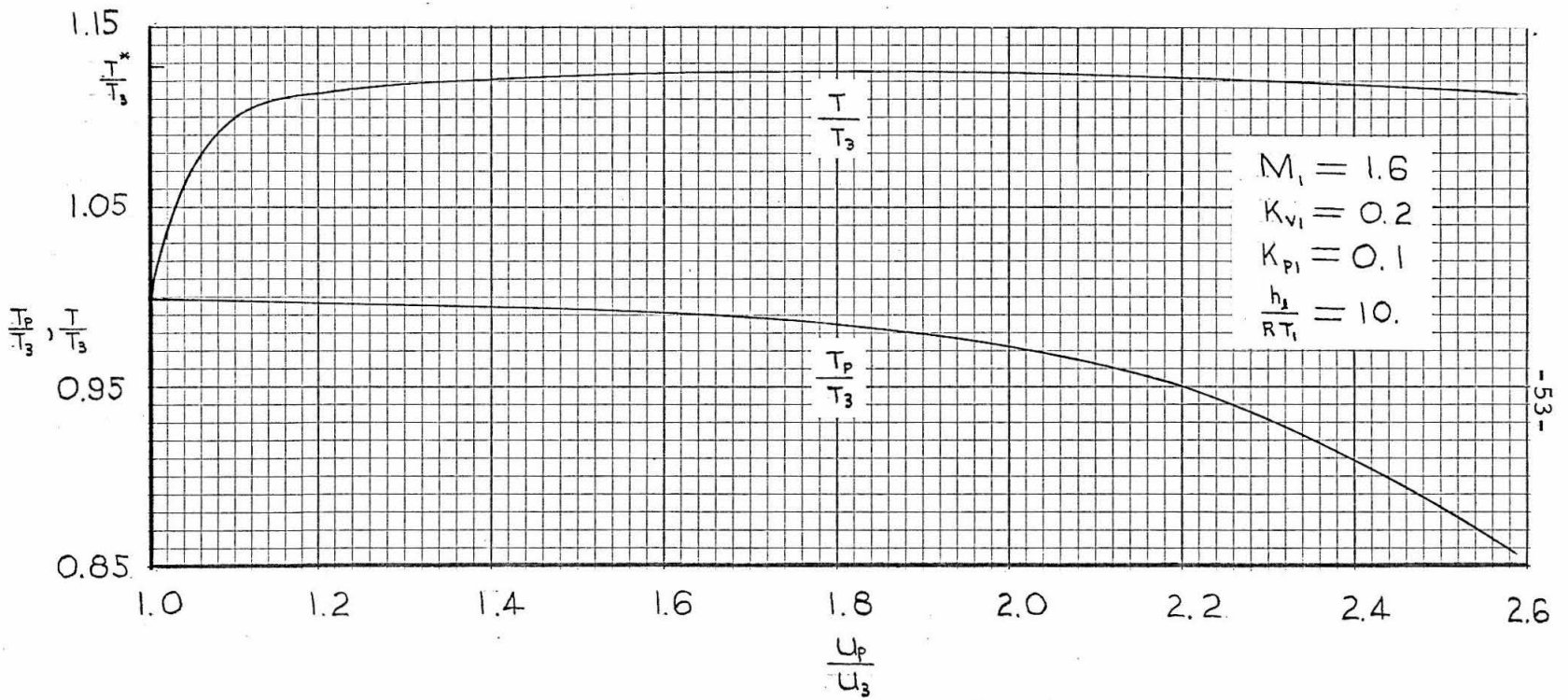

Figure 12. Temperature Equilibration for a Typical Case with $\delta > 1.0$.

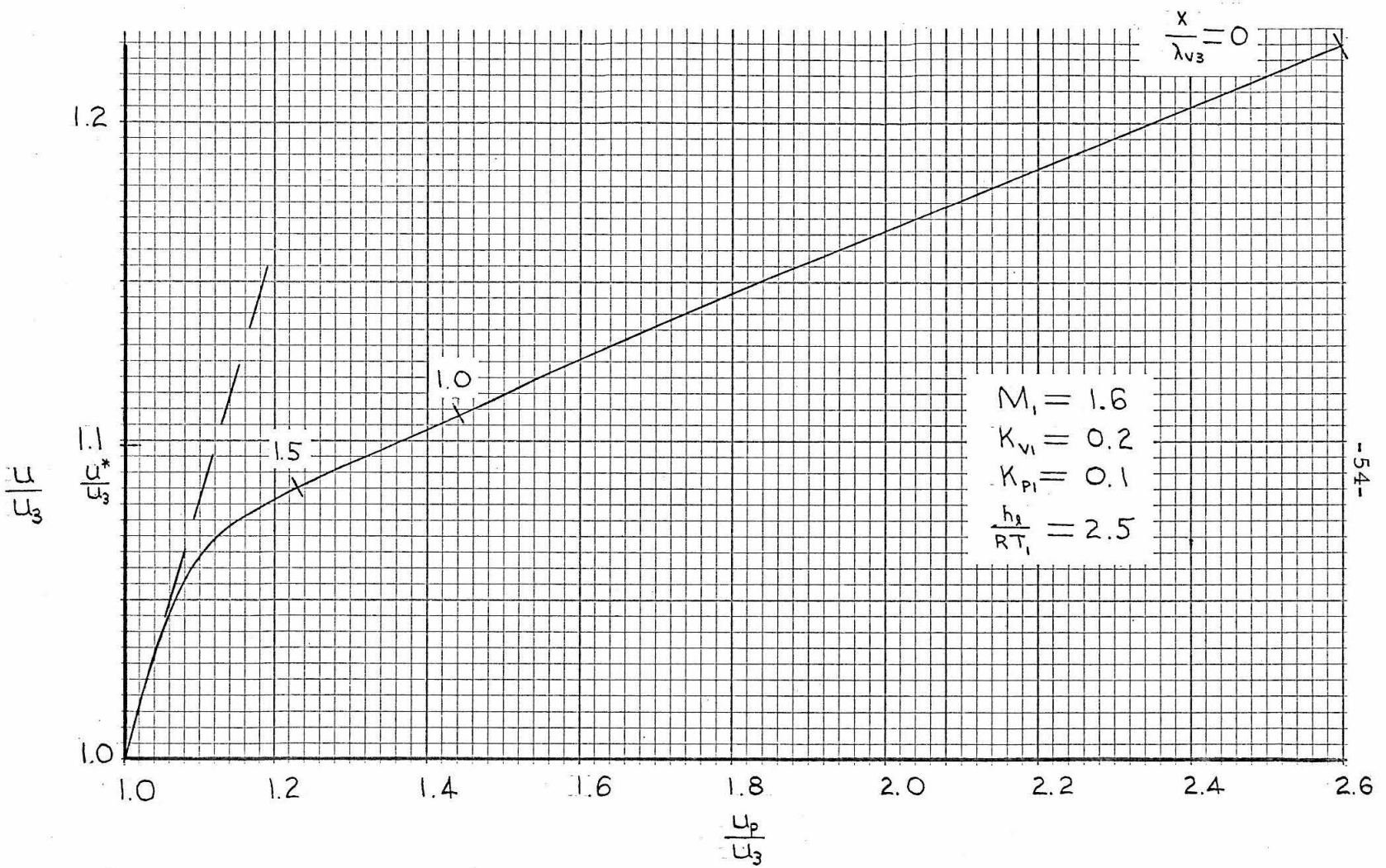

Figure 13. Velocity Equilibration for a Typical Case with $\delta < 1.0$.

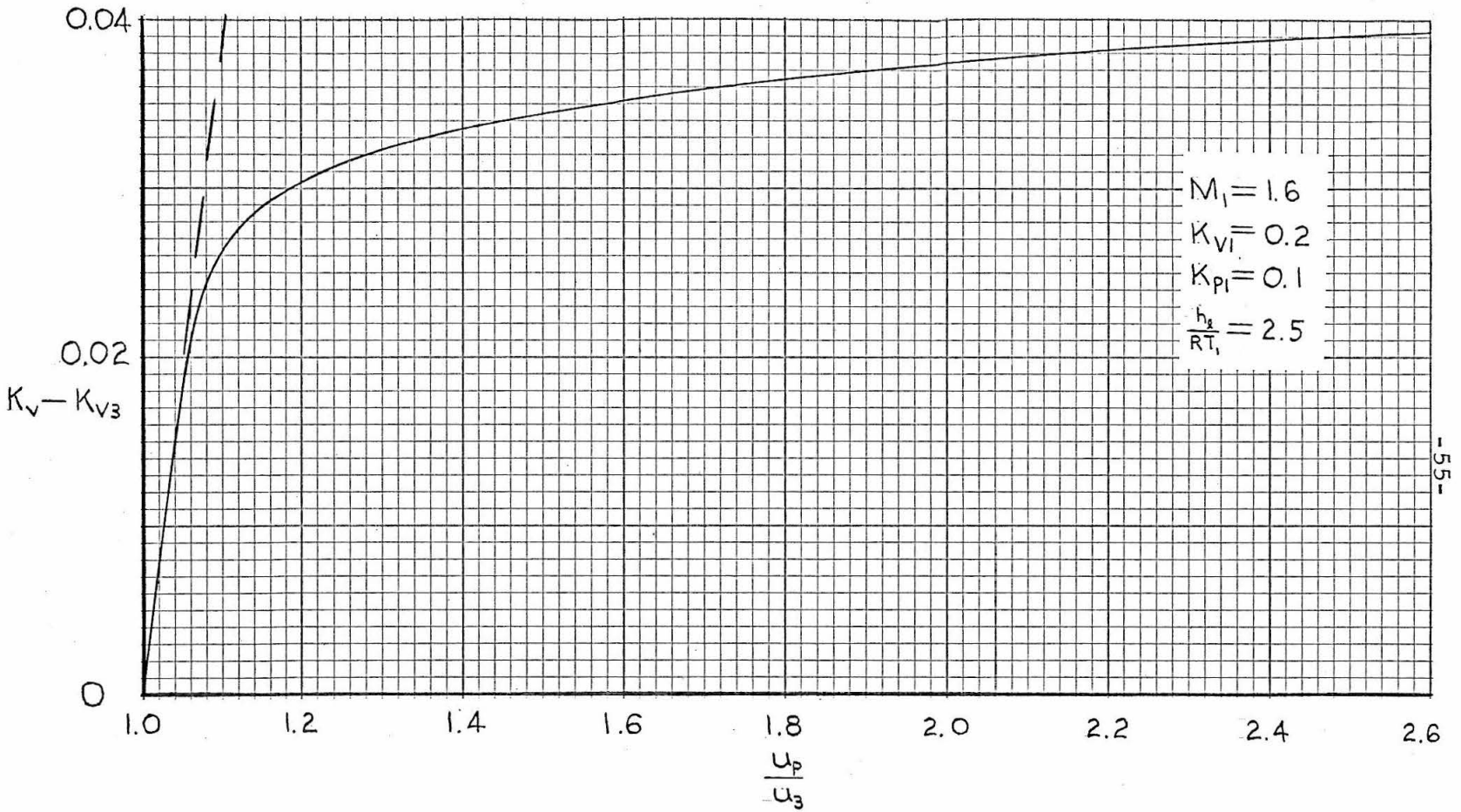

Figure 14. Vapor Concentration Equilibration for a Typical Case with $\delta < 1.0$.

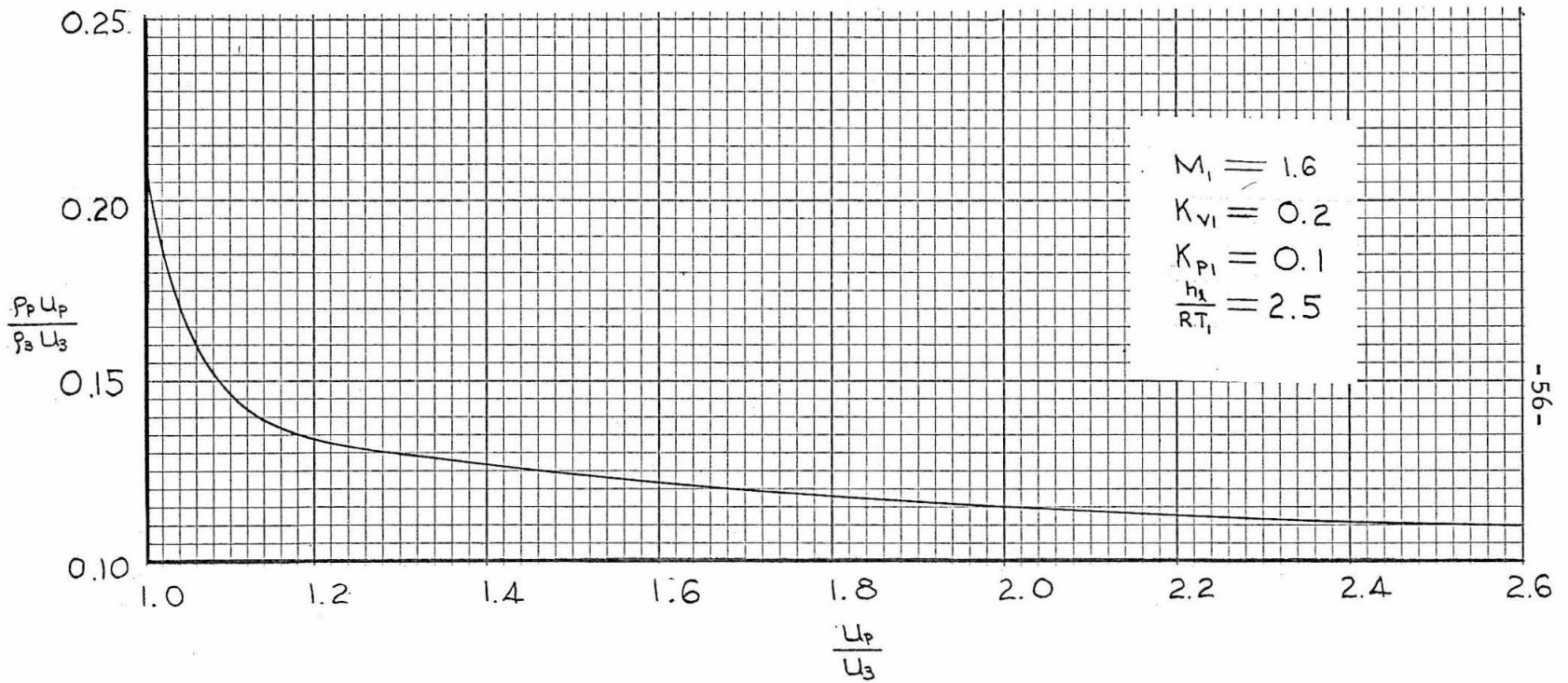

Figure 15. Particle Mass Flow Equilibration for a Typical Case with $\delta < 1.0$.

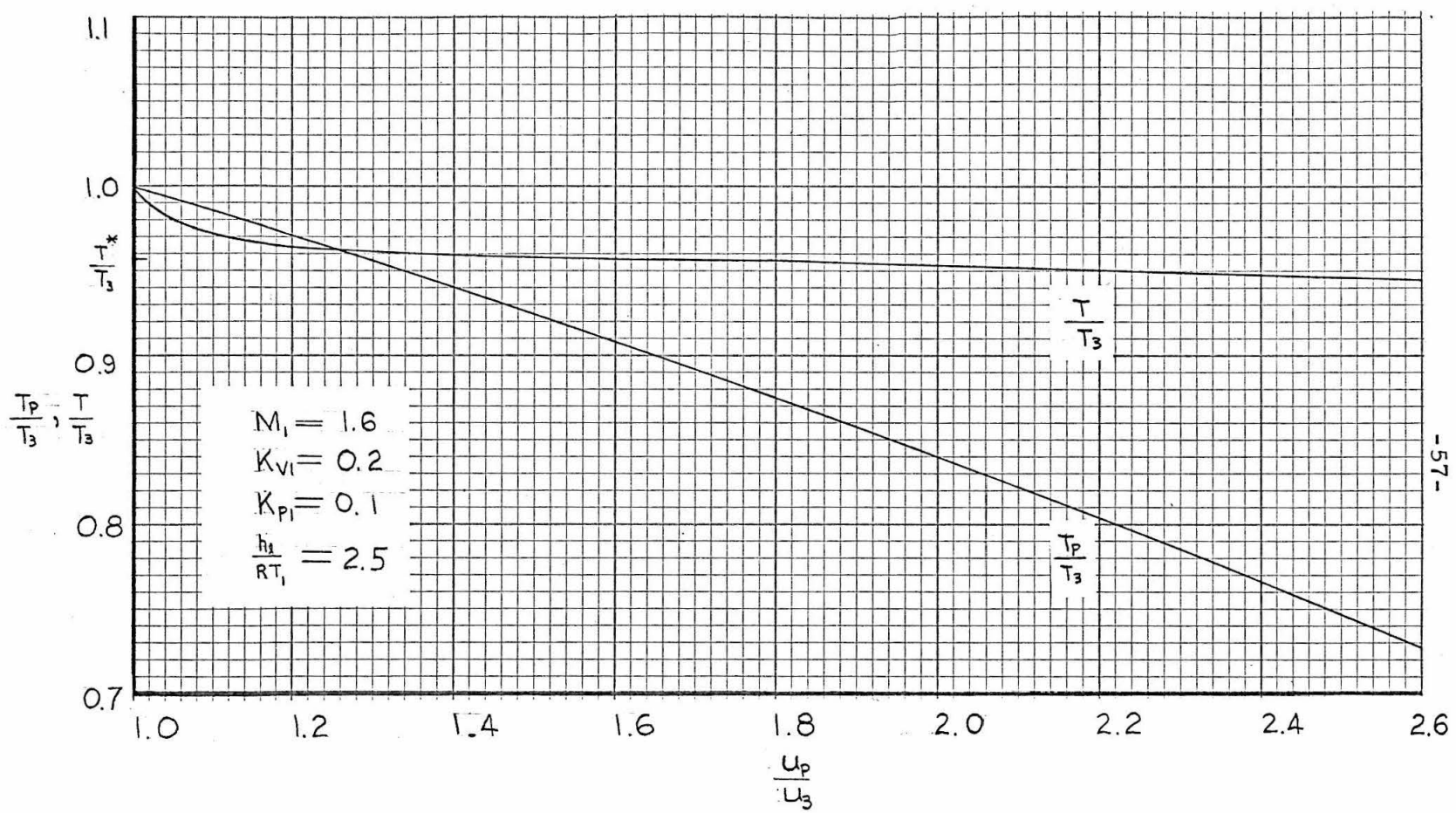

Figure 16. Temperature Equilibration for a Typical Case with $\delta < 1.0$.

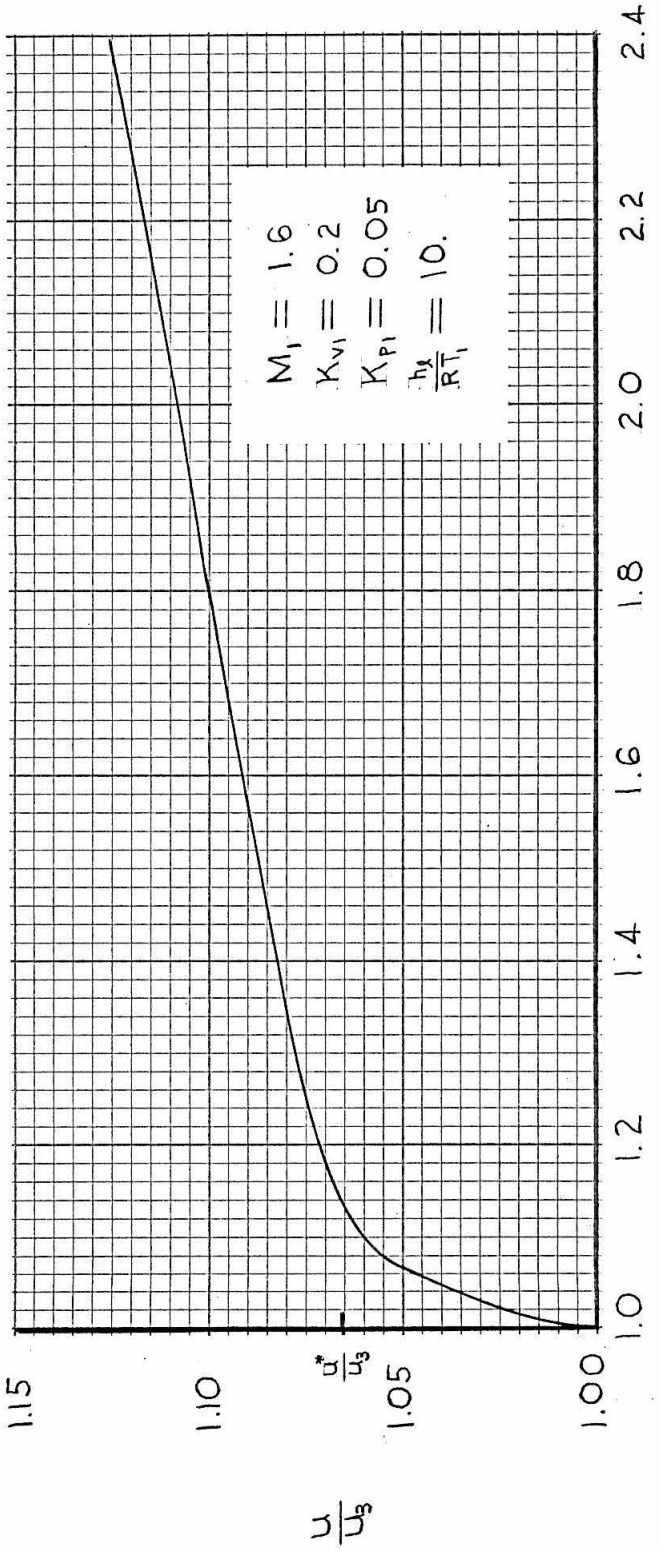

Figure 17. Velocity Equilibration for a Case in Which $K_{p3} = 0$.

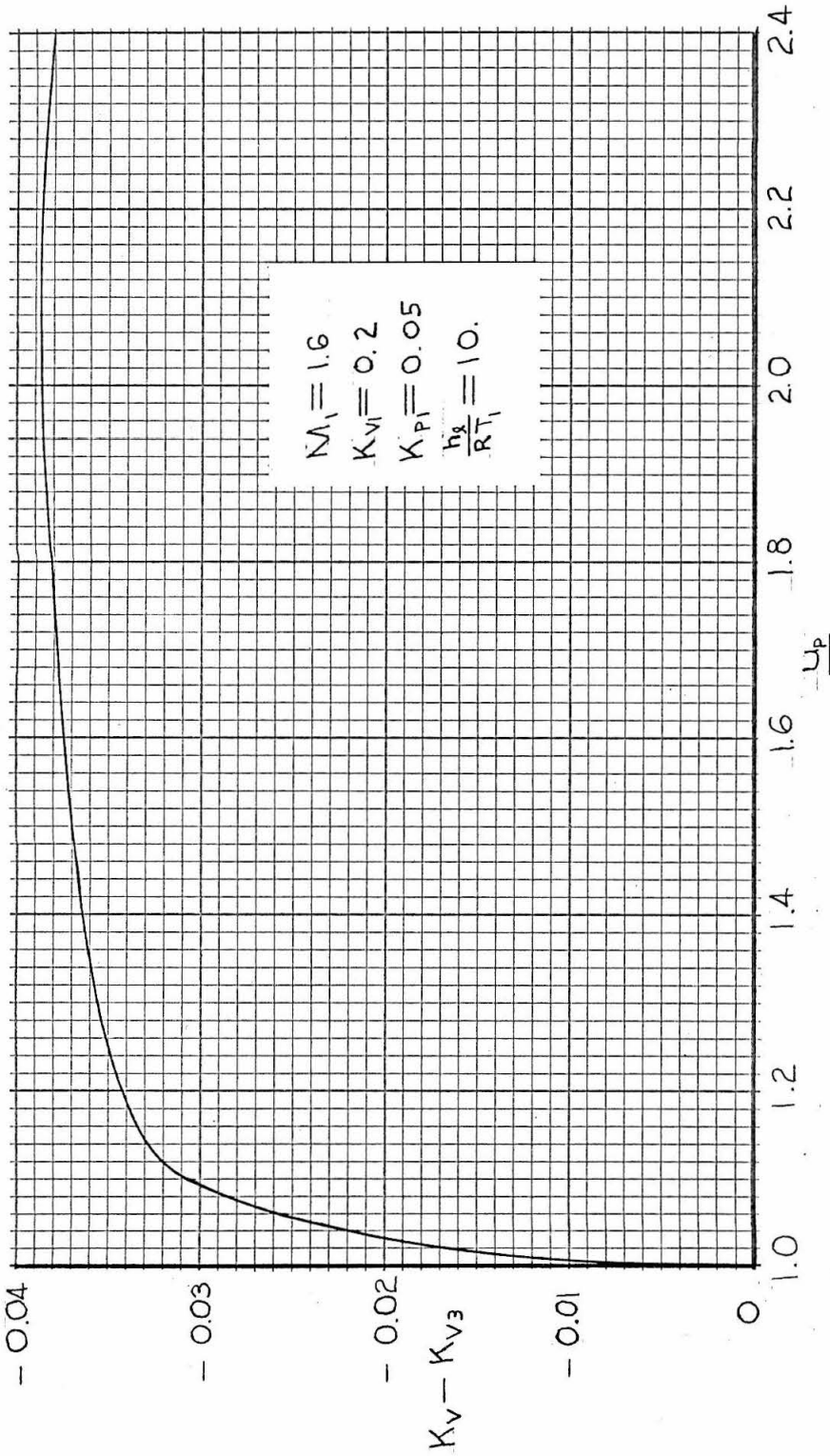

Figure 18. Vapor Concentration Equilibration for a Case in Which $K_{p3} = 0$.

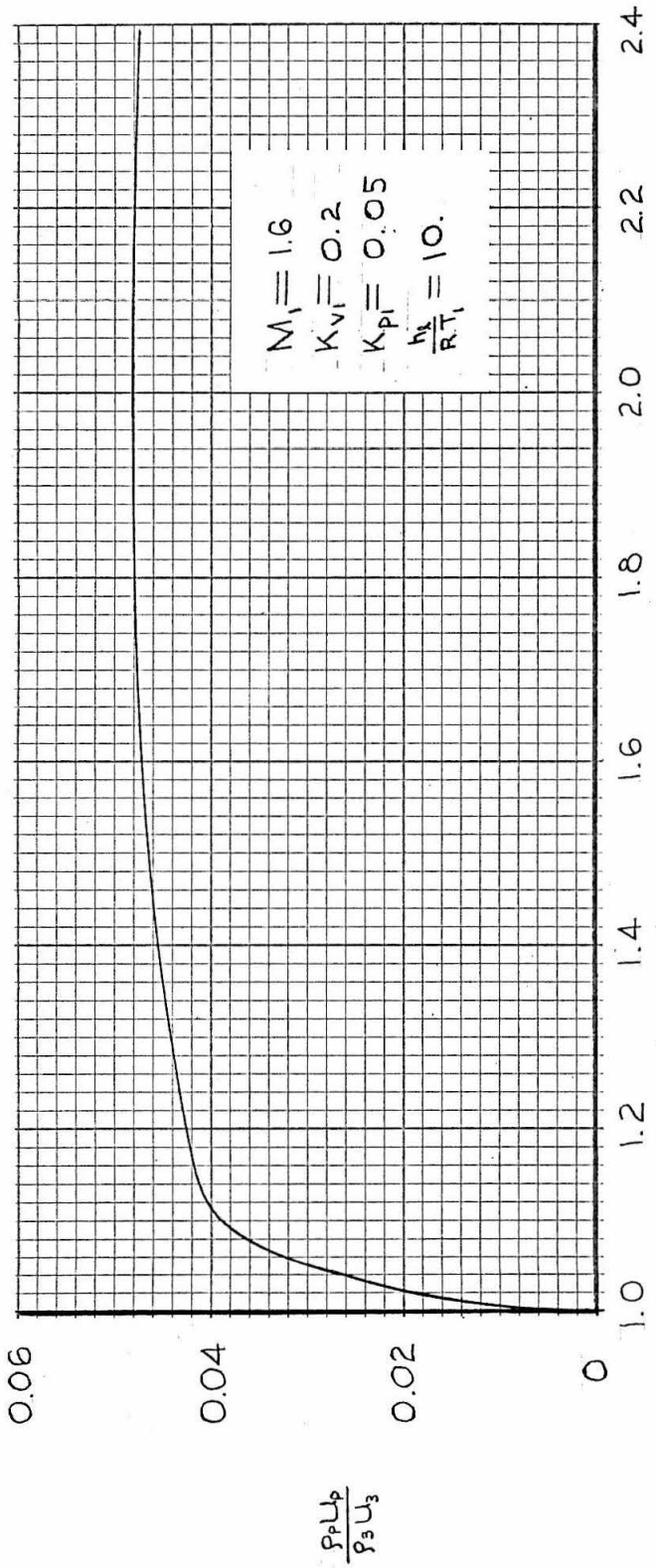

Figure 19. Particle Mass Flow Equilibration for a Case in Which $K_{p3} = 0$.

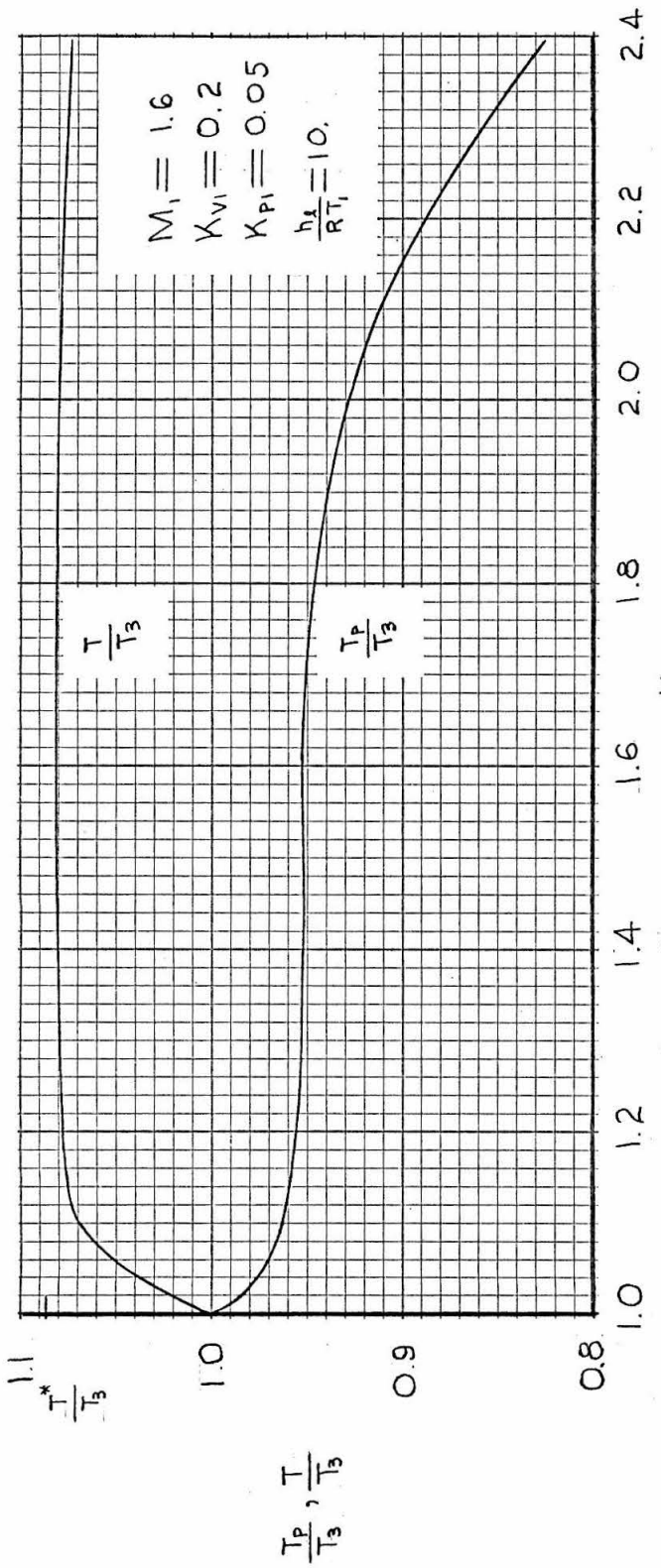

Figure 20. Temperature Equilibration for a Case in Which $K_{p3} = 0$.